PREDICTING BIOLOGICAL DEGRADATION AND TOXICITY OF STEROIDAL ESTROGENS

by

William J. Barr

B.S. Chemical Engineering, University of Pittsburgh, 2005

M.A.T. Secondary Mathematics Education, University of Pittsburgh, 2006

Submitted to the Graduate Faculty of

Swanson School of Engineering in partial fulfillment

of the requirements for the degree of

Master of Science in Civil Engineering

University of Pittsburgh

2011

UNIVERSITY OF PITTSBURGH

SWANSON SCHOOL OF ENGINEERING

This thesis was presented

by

William J. Barr

It was defended on

November 15, 2011

and approved by

Jason D. Monnell, Ph.D., Assistant Professor, Civil and Environmental Engineering Department

Vikas Khanna, Ph.D., Assistant Professor, Civil and Environmental Engineering Department

Thesis Advisor: Willie F. Harper Jr., Ph.D., Associate Professor, Civil and Environmental Engineering Department

PREDICTING BIOLOGICAL DEGRADATION AND TOXICITY OF STEROIDAL ESTROGENS

William J. Barr, M.S.

University of Pittsburgh, 2011

This study was to construct a model to predict a variety of biological transformations of Ethinylestradiol (EE_2) using electronic theory and to analyze the estrogenic potential of EE_2 and its metabolites. As a secondary goal, Frontier Electron Density (FED) theory was applied to the natural steroidal estrogens, estrone (E_1), estradiol (E_2) and estriol (E_3) to determine if similar initiating reactions could be expected. Electron density profiles were calculated for EE_2 metabolites to determine possible metabolic pathways up to the cleavage of the first ring. The pathways predicted in this study assume that enzymes commonly found in wastewater treatment systems will be available to attack EE_2 and each metabolite. Predictive pathways were generated for EE_2 based on the electron density and well established degradation rules. A number of metabolites were shown to be consistent with FED theory.

There are many methods available for effectively calculating the electron density of a given molecule. Calculations were carried out on the Pittsburgh Supercomputer (PSC) using the computational chemistry software Gaussian 03. Two molecular orbital theories available for use in Gaussian 03 were used and results compared to determine if the level of theory significantly affected the accuracy of the electron density calculations. In the beginning of this study only one theory was used but after studying the available theories in more detail I implemented a theory that was shown to be more accurate in literature. Using this information and well established degradation rules, metabolic pathways leading up to the first ring cleavage were predicted. Experimentally measured metabolites appear in the predicted pathways.

In order to evaluate the environmental impacts of steroidal estrogens and their subsequent metabolites the estrogenic potential is calculated using chemaxon software. The estrogenic potential was estimated

for EE_2 and each of its metabolites both predicted and experimental as well as E_1, E_2 and E_3 and known experimentally measured metabolites that are similar to EE_2. In all cases the estrogenic potential of the metabolites indicate that they have a lower toxicity than the parent compounds but may still retain estrogenic potential after biotransformation.

TABLE OF CONTENTS

1.0 INTRODUCTION 1

1.1 ENVIRONMENTAL IMPACT 1

1.2 BIOLOGICAL REMOVAL OF STEROIDAL ESTROGENS 2

1.3 DETECTION OF EE_2 4

1.4 ESTROGENICITY 6

1.5 BIOLOGICAL METABOLITES 10

1.6 FRONTIER ELECTRON DENSITY 11

1.7 FED CALCULATIONS 12

1.8 OBJECTIVES 17

2.0 METHODOLOGY 19

2.1 METHOD DESCRIPTION 19

2.2 FRONTIER ELECTRON DENSITY 20

2.3 DEGRADATION RULES 24

2.4 ESTROGENIC POTENTIAL 26

3.0 RESULTS 27

3.1 FRONTIER ELECTRON DENSITY 27

3.2 INITIATING REACTIONS 28

3.3 THEORY AND BASIS SET COMPARISON 33

3.4 PATHWAYS ... 37

3.5 ESTROGENIC POTENTIAL ... 39

4.0 CONCLUSION ... 42

APPENDIX A ... 44

APPENDIX B ... 50

APPENDIX C ... 51

APPENDIX D ... 54

APPENDIX E ... 74

APPENDIX F ... 79

BIBLIOGRAPHY ... 83

LIST OF TABLES

Table 1. Analysis of Basis Sets 36

Table 2. Analysis of Level of Theory 36

Table 3. Estrogenic Potential analysis for metabolic pathways 40

Table 4. Estrogenic potential analysis of steroidal estrogens and sulfate conjugates 78

Table 5. 2OH-EE_2 pathway information 80

Table 6. 6HCYC-EE_2 pathway information 81

Table 7. SO_4-EE_2 pathway information 82

LIST OF FIGURES

Figure 1. One Electron Hamiltonian 12

Figure 2. HF extension of the one electron Hamiltonian 13

Figure 3. Gaussian 03 input file 21

Figure 4. FED equation 23

Figure 5. Degradation Rules 25

Figure 6. Hydrophobicity of E_2 26

Figure 7. EE_2 with atom labels 27

Figure 8. EE_2 FED at each carbon site 28

Figure 9. Initiating metabolites 29

Figure 10. 2OH-EE_2 compared to EE_2 based on the initial transformation 30

Figure 11. 6HCYC-EE_2 FED compared to the parent compound 31

Figure 12. SO_4-EE_2 FED compared to the parent compound 32

Figure 13. Electron density comparison of basis sets STO-3G vs. 6-31G(D) 33

Figure 14. Theory comparison HF vs. DFT 35

Figure 15. 2OH-EE_2 pathway 37

Figure 16. 6HCYC-EE_2 pathway 38

Figure 17. Gaussian Input Structure 50

Figure 18. Estrogenic Potential: Direct Metabolites 75

Figure 19. Estrogenic Potential: 2OH-EE_2 pathway 76

Figure 20. Estrogenic Potential: 6HCYC-EE_2 pathway 77

ABBREVIATIONS

ACM – Adiabatic Connection Method

AOB – Ammonia-Oxidizing Bacteria

AR – Androgen Receptor

B3LYP - Becke, 3 parameter ACM, LYP

CAFO – Concentrated Animal Feeding Operations

CBR – Conventional Bioreactor

CPRG – Chlorophenol red-β-D galactopyranoside

DFT – Density Functional Theory

ECD – Electron Capture Detection

EDC – Endocrine Disrupting Compound

ELISA – Enzyme Linked Immunosorbent Assays

ERE – Estrogen Receptor Enzyme

E_1 – Estrone

E_2 – 17β-Estradiol

EE_2 – 17α-Ethinylestradiol

E_3 – Estriol

FMO – Frontier Molecular Orbitals

GC – Gas Chromatography

GGA – Generalized Gradient Approach

GR – Glucocorticoid Receptor

H-Bond – Hydrogen Bond

HF – Hartree-Fock

HOMO – Highest Occupied Molecular Orbital(s)

HRGC – High Resolution Gas Chromatography

KS – Kohn Sham

LC – Liquid Chromatography

LOD – Limit of detection

LUMO – Lowest Unoccupied Molecular Orbital(s)

LYP – Lee, Yang and Parr, 1988

MBR – Membrane Bioreactor

MP2 – Moller-Plesset perturbation theory

MR- Mineral Corticoid Receptor

MS-Mass Spectrometry

NAS – Nitrifying Activated Sludge

NCI – Negative Chemical Ionization

PAH – Polycyclic Aromatic Hydrocarbon

PR – Progesterone Receptor

PSC – Pittsburgh Supercomputer

QSAR – Quantitative Structural Activity Relationship

RIER – Redox Induced Electron Rearrangement

SCF – Self Consistent Field

SPE – Solid Phase Extraction

STW – Sewage Treatment Works

TR – Thyroid Receptor

Vg – Vitellogenin

WWTP – Wastewater Treatment Plant

ACKNOWLEDGEMENTS

I would like to thank the National Science Foundation, GEM fellowship and University of Pittsburgh for their financial support. I would like to thank the members of my committee for their guidance in completing this project. I would like to thank Dr. Willie F. Harper Jr., for his invaluable mentorship and patience throughout my time here.

I am thankful for the encouragement and unending support of Dr. Sylvanus Wosu and Alaine Allen who encouraged me to come back to school and continually assisted me in finding funding. I wish to thank my family and friends who has been patient with me as I transitioned from one career to another.

Finally, I give thanks to my Lord and Savior Jesus Christ for grace and mercy throughout this arduous yet fulfilling process.

1.0 INTRODUCTION

1.1 ENVIRONMENTAL IMPACT

Highly active endocrine disrupting compounds (EDC) can be found in the environment as both natural and synthetic steroidal estrogens. Natural estrogens are excreted from the human body in quantities that are still estrogenically active (Aldercreutz 1986). Ethinylestradiol (EE_2), the primary component in birth control pills, is a synthetic estrogen based on estradiol. EE_2 is excreted from the body and primarily reaches the aquatic ecosystem via municipal wastewater as both unused estrogen and as conjugated metabolites. As a result EE_2 has been detected in surface waters that have come into contact with wastewater effluents (Ternes 1999; Kolpin 2002; Kuch and Ballschmiter 2001; Baronti 2000). This has led to the detection of EE_2 in these water bodies in the ng/L concentration range. (Kolpin 2002; Kuch and Ballschmiter 2001; Baronti 2000).

Feminization of male fish has been observed in a number of different studies. Purdom et al. (1994) found that sewage treatment plant effluent had an estrogenic effect on fish. Parkkonen et al. (2000) showed that contraceptive pills which contain EE_2 have an estrogenic effect on fish. Pawlowski et al. (2004) showed that exposure to EE_2 led to gonadal defects in male fathead minnows. Routledge et al. (1998) has shown that exposure to Sewage treatment works (STW) effluent can have an estrogenic effect on trout and roach. Desbrow et al. (1998) has verified the estrogenicity found in wastewater treatment plants (WWTP) can be attributed to EE_2 and the natural steroidal estrogens E_1 and E_2 using the Yeast Estrogen Screen (YES).

1.2 BIOLOGICAL REMOVAL OF STEROIDAL ESTROGENS

EE_2 has been shown to be a powerful EDC and an environmental threat even at trace levels (low ng/L). EE_2 is biodegradable via the activated sludge process. To determine how to improve the biodegradation of EE_2, the current work refers to a number of different studies that have examined different methods of biological removal. Yi and Harper (2007) tested the removal of EE_2 by coupling it with the nitrification process. They used an enriched culture with autotrophic ammonia oxidizers to determine how EE_2 reacted during the nitrification process. Results indicated that EE_2 undergoes electrophilic initiating reactions on the phenolic ring (ring A see appendix A2). Furthermore, they also showed that ring A was the first ring that is cleaved. Shi et al. (2004) further demonstrated the removal of EDCs by carrying out batch experiments using both nitrifying activated sludge (NAS) and ammonia oxidizing bacteria (AOB) where they tested four estrogens and observed the degradation rate kinetics. They concluded that NAS was the more effective method and that E_2 was the easiest to degrade obeying first order reaction rates. In another study involving AOBs and continuous-flow reactors, Khunjar et al. (2011) found that AOBs degraded EE_2 five times faster than heterotrophs. This study also detected the presence of the previously reported sulfo-EE_2 conjugate indicating that it may be recalcitrant. These three studies demonstrated that treatment plants have the capabilities to degrade EE_2. A number of potentially active metabolites have been detected during these studies and authors expressed concerns about the reactivation of inert conjugated estrogens and the estrogenic activity that is retained after treatment is complete.

Other studies have examined the treatment of WWTP effluent using non-conventional systems that ranged from more intensive and costly techniques to systems that could be deployed in developing countries. Shi et al. (2010) investigated the removal of E_1, E_2 and EE_2 in stabilization ponds using algae and duckweed. They used two different enzyme-linked immunosorbent assay (ELISA) methods in conjunction with solid phase extraction (SPE) to measure the estrogens in the ng/L concentration range. The rate of degradation increased when synthetic wastewater was in the presence of duckweed and algae. The degradation of the estrogens was attributed to both biodegradation and sorption with authors stating that sorption occurred early in the treatment process and that sorbed estrogens were subsequently biodegraded by microorganisms, algae or duckweed. Della-Greca et. al. (2008) identified different metabolites using algae including coupled metabolites and a transformation where the active ring was modified. Clouzot et al. (2010) compared the degradation of EE_2 in membrane bioreactors (MBR) using acclimated activated sludge with removal of activated sludge (AS) directly from a wastewater treatment plant. After the acclimated sludge was well established the concentration of EE_2 was controlled to reach 1 mg/L in both vessels. They determined that removal could reach 99% using the acclimated activated sludge and only 88% using standard activated sludge from a wastewater treatment plant. Authors attributed the difference in removal efficiency to the nitrifying capabilities of the system designed in this study. Yi et al. (2011) also tested the removal of EE_2 in an MBR and conventional bioreactor (CBR) at >50µg/L. The MBR was shown to perform better than the CBR because of better sorption to MBR biomass. Both systems were shown to have similar rates of complete mineralization and the MBR biomass was capable of quickly producing metabolites over an extended period of time. This second set of studies indicate that the performance of wastewater treatment plants (WWTP) can be improved by using more advanced wastewater treatment methods but may still result in the production of potentially active metabolites and are often significantly more costly than using conventional methods.

1.3 DETECTION OF EE_2

EE_2 requires analytical techniques with limit of detection (LOD) low enough to measure EE_2 at levels as low as 0.1 ng/L. Huang, 2001 compared the detection capabilities of (Gas Chromatography/Mass Spectrometry) GC/MS/MS to the ELISA method for detecting both E_2 and EE_2 in wastewater effluent and surface water. In conventional wastewater treatment effluent, the remaining endocrine disrupting component was measured at 0.2 and 4.1 ng/L for E_2 and EE_2 respectively. Using reverse osmosis, removal was <0.4 ng/L total between both hormones which is below the LOD. This result indicates that E_2 which is active at 1 ng/L is inactivated but does leaves some doubt about the activity of EE_2 which may be active as low as 0.1 ng/L. This study identified EDC contamination in wastewater effluents at biologically active concentrations and shown the capabilities and limitations of prominent and commercially available EDC detection methods

While WWTPs are capable of removing EDCs the sludge may also be used in land applications and effect feeding operations. Hutchins et al. (2007) analyzed CAFOs to determine the effect of land application as a potential source of estrogen runoff into the environment. To detect free estrogens in their samples they used SPE in conjunction with GC/MS/MS. A different method was used for the conjugates replacing GC/MS/MS with LC/MS/MS. The limit of detection (LOD) was 20 ng/L. In the swine sow lagoon they were able to detect E_1 $E_2\beta$, and E_3 at 9940, 194 and 6290 ng/L respectively. Conjugates of EE_2 have been identified using nitrifying bacteria in activated sludge experiments (Yi 2007) in wastewater samples using the ELISA (Huang 2001) and in sewage and river waters using SPE/LC/MS (Gentili 2002). In most cases Hutchins et al. detected less than 1 ng/L of conjugated steroidal estrogens in runoff.

Wastewater effluent can come into contact with surface waters and find their way to drinking water. Kuch and Ballschmiter (2001) detected steroidal estrogens among other potential non-steroidal EDCs in a number of different types of waters including surface and drinking water. Detection was done using high resolution GC negative chemical ionization MS (HRGC-NCI-MS) and confirmed using a similar method but replacing NCI with ECD. The LOD for this technique is 50 pg/L in drinking water and 200 pg/L in sewage water effluent. The concentration ranges for steroidal estrogens were 200 pg/L to 5 ng/L and 100 pg/L to 2 ng/L in surface waters and drinking waters respectively.

There are a number of difficulties associated with the detection of steroidal estrogens at the lower end of the active concentration range. Many methods exist for detection but frequently utilize chromatography and mass spectrometry individually or in tandem. In any case the aforementioned combination requires skilled personnel and very expensive equipment. Hintemann et al. (2006), in an attempt to assuage many of the difficulties associated with the detection of EDCs, developed two immunoassays for detecting E_2 and EE_2. Both methods were ELISAs and were optimized based on previous studies to allow for the broader use of the methods. The LOD for E_2 and EE_2 were 0.05 ng/L and 0.01 ng/L respectively. The concentrations detected for E_2 and EE_2 were 12 and 1.8 ng/L in effluent and 4 and 0.7 ng/L in surface water respectively. In each of these studies, despite the extremely small concentrations detected, EE_2 was frequently detected at concentrations known to exert estrogenicity on biological systems.

1.4 ESTROGENICITY

The toxicity of steroidal estrogens is based on the estrogenicity that they exert upon the environment where they are located. Estrogenicity is the result of an estrogenic compound first interacting with the estrogen receptor enzyme (ERE) and causing the enzyme to yield some biological activity. This can include the production of female hormones Vitellogenin (Vg) and the growth of female hormonal parts such as ovaries. These potent EDCs become hazardous when excreted from the body or after synthetic drugs designed to specifically affect the endocrine system are disposed of unused. In order to determine the extent to which these compounds retain their estrogenicity a number of methods have been developed based on the effect of known estrogenic molecules. Routledge and Sumpter (1996) developed a method that has become widespread for measuring estrogenicity. This method involves a recombinant yeast strain (Saccharomyces cerevisiae) that has the human estrogen receptor integrated into it. With this gene the expression of β-galactosidase is controlled by the ERE. When estrogenic activity takes place β-galactosidase is excreted into the system. In this method β-galactosidase causes a color change with a color changing agent known as Chlorophenol red-β-D galactopyranoside (CRPG) that will turn the solution from yellow to red. Using spectrophotometry, the level of estrogenic activity can be calculated based on the amount of β-galactosidase released. A blank, containing only deionized water, is used and set at 0 and the natural steroidal estrogen E_2, one of the most potent estrogens, is used as the standard. They did not actually look for steroidal estrogens but rather the estrogenicity of surfactants. However, this method known as the YES screen has become prominent in the wastewater community for testing wastewater samples.

Gibson et al. (2005) analyzed fish bile that has been exposed to WWTPs to determine the level of estrogenicity and identify specific contaminants. HPLC-SPE was used to get quality readings of fish bile and compared fish exposed only to tap water and fish exposed to EDC containing WWTP effluent. The YES method was implemented as developed by Rougtledge and Sumpter (1996). E_2 was detected in the ng/L concentration range in fish that were exposed to tap water. In fish bile where estrogenic activity was detected E1, E2, EE2 and a number of nonylphenolics were detected in the low ng/L and pg/L concentration ranges.

There are a number of other methods that have also been developed to calculate the estrogenicity of not only steroidal estrogens but in other contaminants such as xenobiotics. Nishikawa et al. (1999) developed a system not only to test estrogenicity but to test the effect of toxicants on other receptors including the androgen, progesterone, and thyroid hormone receptors (AR, PR and TR respectively). This assay employs a two hybrid assay that uses coactivators known for receptor expression that come from actual mammals as opposed to recombinant yeast. The test is able to identify which receptors are affected by which chemicals based on known results. Instead of using yeast, they use coactivators that have been derived from mammals to get more genuine results and avoid interferences by unknown factors. This method has a lower sensitivity than the YES assay.

Another method was used to measure estrogenicity by measuring the production of an actual hormone instead of using an assay to find an additive as an indicator. Shilling and Williams (2000) implemented a method using cut liver slices and the induction of Vitellogenin Vg. They were able to demonstrate the level of estrogenicity expressed in vitro by E_2 by exposing liver slices to 1000 nM of E_2. They also tested the estrogenicity of two weak environmental estrogens over the concentration range of 0 to 250 μM. The two contaminants tested were o.p. DDE (2-(2-Chlorophenyl)-2-(4-chlorophenyl)-1,1-dichloroethene) and bisphenol A. They show that both contaminants have an EC50 value at least 4 orders of magnitude lower than E_2. These studies have shown that it is possible to measure estrogenicity using a number of methods and to determine the relative estrogenicity of a number of different contaminants. However, many of these methods, much like the detection of EDCs require significant amounts of time and highly skilled personnel.

It has been shown that measuring the estrogenicity of a molecule is not a trivial matter and could potentially be costly in both time and money. Fang et al. 2001 studied natural and synthetic steroids to determine what structural properties contribute to estrogenicity. They utilized a QSAR model to analyze 230 molecules (with and without phenolic rings) and they found that the number of hydrogen bond (H-bond) donating groups (n_d) correlated negatively with estrogenicity. They also found that the octanol-water partitioning coefficient (log P) was positively correlated with estrogenicity. Lipinski et al., 2001 found similar results for their analysis of approx. 2500 organic compounds. Schultz et al., 2001 developed structure-activity relationships for 120 aromatic compounds and found that n_d correlated well with estrogenicity but hydrogen bond accepting groups (n_a) had a negative correlation. They also determined that the hydrophobicity of rings B, C, and D (but not A) was positively correlated with estrogenicity. These parameters (log P, n_d, n_a) can be determined from the chemical structures using computational chemistry methods and understanding of which functional groups are capable of hydrogen bonding.

In order to determine the parameters that will affect estrogenic potential it is necessary to understand the mechanism of estrogenicity in terms of how the ligand binds to the receptor. E_2 was used as the standard for estrogenicity as is the case with laboratory estrogenicity tests first performed by Routledge and Sumpter (1996) for developing the YES assay. The estrogen and receptor interactions are governed partially by the hydrogen bonding properties of the ligand and the hydrophobicity (Waller et al. 1996; Schultz et al. 2002). Hydrogen bond donor groups interact with the binding domain of the estrogen receptor and hydrophobicity relates to the potential of the molecule as a whole to contain some level of estrogenicity with no regard to potency.

Hydrogen bond acceptor groups must be considered as they can form intramolecular hydrogen bonds with donor groups. This interaction may affect the ability of the donor group to interact with the receptor. In determining receptor interactions for drugs in general, Lipinski et al. (2001) indicated that hydrogen bond acceptors must be considered when attempting to computationally quantify hydrogen bond donor strength. Saliner et al. (2003) attempted to use a pharmacophore model to predict the estrogenic activity of 120 aromatic chemicals. They separated the analyzed molecules into active and inactive and used quantum similarity methods to determine what functional groups made certain ligands active with the human estrogen receptor. However, four compounds were misidentified as active by their model. They hypothesized that this may be a result of intramolecular hydrogen bonding which their pharmacophore model does not consider. Based on the literature and experimental data the three properties H-bond donors, acceptors and hydrophobicity provide a framework for predicting estrogenic potential.

1.5 BIOLOGICAL METABOLITES

Biodegradation has been shown to occur in wastewater treatment plants (Baronti 2000, Andersen 2003). Yi and Harper (2007) and Gusseme et al. (2009) have examined biotransformation of EE_2 using nitrifying bacteria and identified a number of metabolites for EE_2. Yi and Harper (2007) identified three different metabolites including one metabolite with the phenolic ring cleaved. Pitak et al. (2008) examined a number of different studies using multiple environments to detect metabolites of both estradiol (E_2) and EE_2 degradation. The biodegradation methods include activated sludge, ammonia oxidizing bacteria, nitrifying activated sludge and microalgae. Transformation products differed dramatically based on the system that was used for degradation. Metabolites involved addition reactions, conjugations on the phenolic hydroxyl group, shifting of the π bonds within the aromatic ring resulting in a loss of aromaticity and ring cleavage. The significance in determining the transformations associated with the steroidal estrogens is an important part of the discussion on toxicity.

For the most part, the primary focus has been the parent compounds and needs to be expanded to include metabolites that may retain estrogenicity. When examining the toxicity of the steroidal estrogens, ring cleavage is a critical step in transformation pathways because "de-ringed" structures are easier to assimilate (Lehninger 1999) and without rings, metabolites are unlikely to bind to estrogen receptors (Fang 2001). A number of studies have detected ring cleavage showing both ring A and ring B cleavage. Yi et al. (2007) and Khunjar et al. (2011) both reported metabolites that show that ring A is the first to be cleaved during biotransformation. While Haiyan et al., 2007, based on the daughter products they detected, proposed ring B cleavage occurred first. This previous research raises the question of whether ring A or B is cleaved first.

1.6 FRONTIER ELECTRON DENSITY

Frontier Electron Density (FED) has received considerable attention within the computational chemistry community for predicting reactivity. The current work aims to apply FED theory to explore EE_2 biotransformation. FED calculations were used elucidate the fundamental principles governing EE_2 reactivity by predicting which positions on the molecule will most likely undergo electrophilic attack.

Fukui et al. (1952) established the use of FED theory by explaining the role of frontier molecular orbitals (HOMO and LUMO) in regards to the reactivity of aromatic hydrocarbons. After validating the theory with experimental data, Fukui further goes on to explain its validity. This study explained the critical importance of electrons in the frontier molecular orbitals (FMO) as the key factors governing the reactivity of active sites for electrophilic, nucleophilic and radical reactions. Electrophilic reactions, which involve an electron-poor molecule attempting to react with the substrate, examine the electron density for the HOMO electrons because of the electrophiles attraction to electrons and the ease of access to those electrons in comparison to all other electrons in the molecule.

Liu et al. (2000) calculated the FED for the dye alizarin red in the presence of a TiO_2 catalyst and compared those results to experimentally determined byproducts. They were able to show that the initiating photo oxidation took place at the highest FED carbon site but that the intermediate was unstable and so a subsequent molecule in the degradation process was detected. Lee et al. (2001) applied Fenton oxidation to five recalcitrant PAHs and identified the oxidation products using GC/MS. Frontier electron density was calculated for each PAH and compared to the oxidation products to determine if the experimental results agreed with the theory. It was shown that four of the five PAHs did agree with FED theory. Ohura et al. (2005) examined airborne PAH's and determined that abiotic chlorination of these molecules coincided with high FED positions. Wang et al. (2007) showed that photo degradation of bis (4-hydroxyphenyl)ethane could be enhanced under UV irradiation in the presence of β-cyclodextrin. The improved removal was associated with certain reaction sites having higher electron density when preceded by UV irradiation. This led to a more than 50% increase in photo degradation. Although these previous attempts focused on abiotic reactions, they bolster the potential for predicting biological oxidations in the same way. Previous efforts to conduct a priori predictions of biodegradation have been very successful when focusing on readily degradable substrates (e.g. glucose) that enter well-characterized metabolic pathways (e.g. glycolysis). FED-based techniques present the promise of predicting biodegradation on complex organics like EE_2; a contribution here can eventually make a significant impact.

1.7 FED CALCULATIONS

Calculating the FED requires the use of well-defined quantum chemistry theories and calculation techniques. The first equation is the one electron Hamiltonian as defined by the equation below (Figure 1). This equation is used in conjunction with the Schrodinger equation to calculate the energy of each electron in a system (atom or molecule).

$$h_i = -\frac{1}{2}\nabla_i^2 - \sum_{k=1}^{m} \frac{Z_k}{r_{ik}}$$

Figure 1. One Electron Hamiltonian

In this, equation the ∇ represents the laplacian operator, m represents the total number of nuclei. Z_k is an atomic number and r_{ik} is the distance between nuclei i and k. This equation must satisfy the following: $h_i\psi_i=E_i\psi_i$. E is the energy eigenvalue and ψ is an eigenfunction that satisfies this equation known as the Schrodinger equation. This equation does not account for interaction potentials between the electron in question and other electrons in the system. This equation underwent two extensions that allowed for easier solutions and for an additional term to represent that potential. These extensions make up what is known as the Hartree-Fock (HF) theory and modifies the one electron Hamiltonian into the following equation:

$$f_i = -\frac{1}{2}\nabla_i^{\,2} - \sum_{k=1}^{nucleii} \frac{Z_k}{r_{ik}} + V_i^{HF}\{j\}$$

Figure 2. HF extension of the one electron Hamiltonian

The additional term in this equation is the interaction potential between the electron in question and other electrons occupying orbital j. This extension also involved the validation of extending this equation to a many electron eigenfunction in what is known as the "Hartree Product" This extension is a critical factor in improving the use of quantum chemistry in defining molecular orbitals and further solving the Schrodinger equation.

Solving the above equations is not a trivial task and has led to consistent development and extension of computational chemistry software packages and theory. One such approach was proposed by Hartree in 1928 (Cramer 2002) known as the self-consistent field method (SCF). This method involves estimating what the eigenfunction will be followed by solving the Schrodinger equation and calculating a second eigenfunction. This function becomes the new estimate and the process is repeated until the calculated eigenfunction converges on the estimated eigenfunction. This process has two primary limitations when it comes to computational chemistry software. The first problem occurs when the initial estimation calculates an eigenfunction that is drastically different and then the second eigenfunction reports a different solution that is drastically different from the second. In this case the software will continue to attempt to find a solution but will not converge and yet will keep attempting to solve until the program reports an error, the computer fails to continue or the time allotted expires and reports the job as being in the middle of processing though it may never finish. The second problem occurs when the first eigenfunction reports a second eigenfunction and in the second iteration the second eigenfunction reproduces the first eigenfunction leading to another infinite and undetectable loop in the SCF method.

In density functional theory electrons interact with one another and with an external potential. The nature of the external potential depends on the constituent being examined. In terms of molecules the external potential is electrons attraction to the nuclei. This interaction has been defined in earlier theories. A major breakthrough in density functional theory is the revelation of the Kohn-Sham (KS) theory. As in the case of the Hartree-Fock theory, DFT was still limited by the difficulty in computing a real interacting system. KS theory defines a new type of molecular orbital where a non-interacting system is equated to a real system with electron interactions. It is noteworthy to mention that KS theory has a number of similarities to the earlier HF theory. Determination of the KS orbitals continues in the same manner as molecular orbital theory by defining the orbitals in a basis set of functions. The kinetic energy and nuclear interaction terms are also identical to those seen in the Fock matrix from HF theory. Solution of the KS orbital also requires an SCF method. However, there is a critical difference between the two theories; DFT has no approximations. The final obstacle to overcome is to relate the exchange energy to the electron density.

The exchange correlation (E_{XC}) has two features. First it is the difference between the classical and quantum mechanical electron-electron repulsion. Second it is the difference between the kinetic energy of the fictitious non-interacting system and the real system. The second portion of E_{XC} is not solved explicitly. Different theories alleviate this deficiency in different manners. In some cases it is ignored in others it is introduced as an empirical parameter. In order to determine E_{XC} the generalized gradient approach (GGA) came to the forefront. The most popular method for determining the exchange functional is the Becke method (1988). For the GGA of the correlation functional the LYP method (1988) is most widely used (Cramer 2002). This method calculates the full correlation energy. The exchange correlation calculations were extended when the extent to which electrons interacted with one another was quantified. This was done using the Adiabatic Connection Method (ACM). Becke optimized this method using 3 parameters in EXC calculations. The ACM method is then applied to the exchange and correlation functional and in our case becomes the B3LYP which is one of the most commonly used theories in computational chemistry.

To analyze the primary differences between the two functions, Cramer compares the method that both DFT and HF use for measuring molecular properties and the calculations of a number of different properties for accuracy analysis. The first major difference is the use of wave functions for HF and electron densities for DFT. This difference is critical because there are semi-empirical components in the HF theory that are not present in DFT. This means that the property being calculated must depend on the electron density which is specifically the case here and so that limitation to DFT is not relevant in this study. The difference between the two types of orbitals used for calculations is the primary reason for shifting from HF to DFT. The KS orbitals used in DFT are similar to the HF orbitals but do not suffer from excessive energy calculations introduced to HF theory because of the way the external potential is calculated. In the case of the KS orbitals all electrons experience the same external potential whereas certain orbitals in HF theory feel the external potential as if an additional electron was added to the molecule. This overestimates energy in HF theory in a manner not seen in DFT. Many molecules were measured using both to compare the results between the two at the same basis sets but the majority of the molecules were analyzed using DFT.

The second major specification that must be made is the basis set to use. A basis set is a mathematical description of orbitals in a system used for theoretical calculations and modeling. Molecular orbitals are represented by equations that will be present in the function representing nodal surfaces (places where the orbital changes signs). The functions that are used are a combination of atom-centered basis functions. The equations use hydrogen atomic orbitals as a foundation but this leads to extremely complex integrals that are too time consuming to solve. This difficulty led to the use of Cartesian Gaussian functions centered on the nuclei. These functions act similar to the hydrogenic atomic orbitals with the exception of an overly ambitious decrease near the nucleus. To account for this linear combinations are used to imitate the atomic orbital behavior. For example, the basis set STO-3G uses a linear combination of three Gaussian equations for the description of the slater type orbitals. STO-3G is a minimal basis set where one basis function is selected for every atomic orbital that is required. In the case of a methane molecule for example this would involve 4 basis functions for hydrogen (1s orbital X 4 molecules) and 5 basis functions for carbon (1s, 2s, 2px, 2py and 2pz X 1 molecule) for a total of 9 basis functions. 6-31G(D) is a split valence basis set with polarization. This means 6 Gaussians are used for non-valence orbitals and then valence orbitals are contracted into two orbitals with the inner orbital employing three Gaussians and the outer orbital using one

Gaussian. An additional set of d-type functions are added to any non H atoms. These functions give a better description of the orbital distortion caused by polarization affects. For example instead of rigidly forcing the shape of a p-orbital to remain unchanged, adding the d-orbital allows a shift in the orbital shape away from what a perfect p-orbital should be. This addition greatly increases the accuracy of bond angles and lengths. Examples of other split basis-sets include 4-31G and 3-21G. (Handbook of Gaussian Basis sets, 1985). The basis sets are affected by the theory in terms of computational cost but based on the different theories and basis sets used it is the basis set that is the primary deciding factor in the length of time for running jobs using Gaussian '03.

1.8 OBJECTIVES

This research is design to assuage the process of identifying environmental toxicants using computational chemistry as a predictive model for the degradation of steroidal estrogens. Experimental techniques are necessary for identification and determining the effect of EE_2 on the environment but these techniques are often extremely costly, difficult and require a significant amount of time and resources. Coupling experimental techniques with the research done in this study will ease the burden of experimental work by explaining current experimental results and predicting potential results. The hypothesis of this study is that biological oxidation will occur at high FED carbon sites. It has been shown in a number of studies that the phenolic ring is often susceptible to electrophilic attacks. FED theory has been used to predict the reactivity of a number of non-substituted aromatic hydrocarbons as well. Non-specific Oxygenase enzymes are present in wastewater treatment systems and are capable of initiating electrophilic substitution on substrates in the system. EE_2 would be a prime candidate for these enzymatic attacks and the nature of this potential reaction fits within Fukui's theoretical basis for the frontier electrons being the critical factor in electrophilic attacks (1952).

The objectives of this study are as follows:

- Use FED theory to predict initiating reactions involved in EE_2 transformation
- Investigate different computational chemical methods for calculating FED
- Generate predictive pathways up to the ring cleavage phenomenon for EE_2
- Analyze the estrogenic potential of the steroidal estrogens and metabolites

2.0 METHODOLOGY

2.1 METHOD DESCRIPTION

Three primary methods have been used in order to analyze the reactivity and toxicity associated with the steroidal estrogens. FED calculations are carried out using Gaussian 03 on the Pittsburgh Supercomputer (PSC). Gaussian 03 is a versatile computational chemistry software package that allows for a number of different calculations using a vast array of different theories and the freedom to define molecular orbitals to the specific intent of the researcher. Jobs can be inserted into Gaussian 03 using a number of different methods that will be discussed in detail in a later section.

Well-established degradation rules are used in conjunction with FED theory to determine what types of reactions will take place at the identified reactive location. These rules are applied to the steroidal estrogens and used in conjunction with FED theory to validate the use of frontier electron density and to generate metabolic pathways up to the ring cleavage. Validation will be determined based on the hypothesis that high electron density carbon sites have a significantly higher probability of being attacked by enzymes that are commonly present in wastewater treatment systems. The common enzymes that were used are the oxygenase enzymes. Other enzymes that may have a significant affect specifically on the metabolites discussed in this study are deconjugation enzymes such as sulfatase enzymes. All of the steroidal estrogens were analyzed to determine the affect the ring D-functional group has on the four steroidal estrogens in terms of estrogenicity and reactivity. Metabolic pathways will be generated up to the ring cleavage metabolite for all EE_2.

When evaluating the environmental impacts of EE_2 it is necessary to determine the estrogenicity. The estrogenic potential is the ability of a molecule to interact with the ERE and was estimated for every molecule in this study based on the known estrogenicity of the parent compounds and specific metabolites found in nature. Estrogenic potential does not account for the biological activity that occurs after the estrogen binds to the ERE. The toxicity of EDCs is based on receptor interactions, specifically ER in this study but this analysis could have potential bearing on other prominent receptors that may be interacted with by toxicants. When an estrogen does interact with the estrogen receptor certain estrogenic activity takes place. Male fish exposed to EDC contaminated water have been shown to produce proteins typically produced only in females (Shillings and Williams 2000) is a primary example. There has also been evidence of intersex fish (Gibson 2005) when exposed to EDC exposed effluent. The goal of this section is to predict the extent to which each metabolite and parent compound is capable of reacting with the ER based on known factors affecting estrogenicity.

2.2 FRONTIER ELECTRON DENSITY

After selecting a theory and basis set based on computational chemistry literature, calculating the energy eigenfunctions requires two steps; first, optimization to the lowest energy conformation and then the actual energy calculation. Figure 3 shows an example input file made using notepad. For ease of explanation this file was made using CO_2. There are a number of different sections to be specified in the Gaussian 03 input file. The first section, the %section is file specifications where a checkpoint file is specified for storing the processes that take place in all calculations relevant to the job being run. This is also where the computer memory and number of processors to be used is specified. The route section is where the job specifications are entered. The third section is the title of the molecule. The fourth section defines the charge of the molecule (specifically if radicals are used) and the spin multiplicity of each atom in the molecule. The final section is where all molecular data is presented including connections, estimated bond lengths and bond types. The size of the molecule being calculated in Gaussian 03 depends tremendously the size of the input file, the time of calculation, the size of the output file and the number of iterations required for completing each objective. None of the specifications used in this study are present in the example file. Appendix 1 contains certain complete input files to give readers an idea of what input files look like.

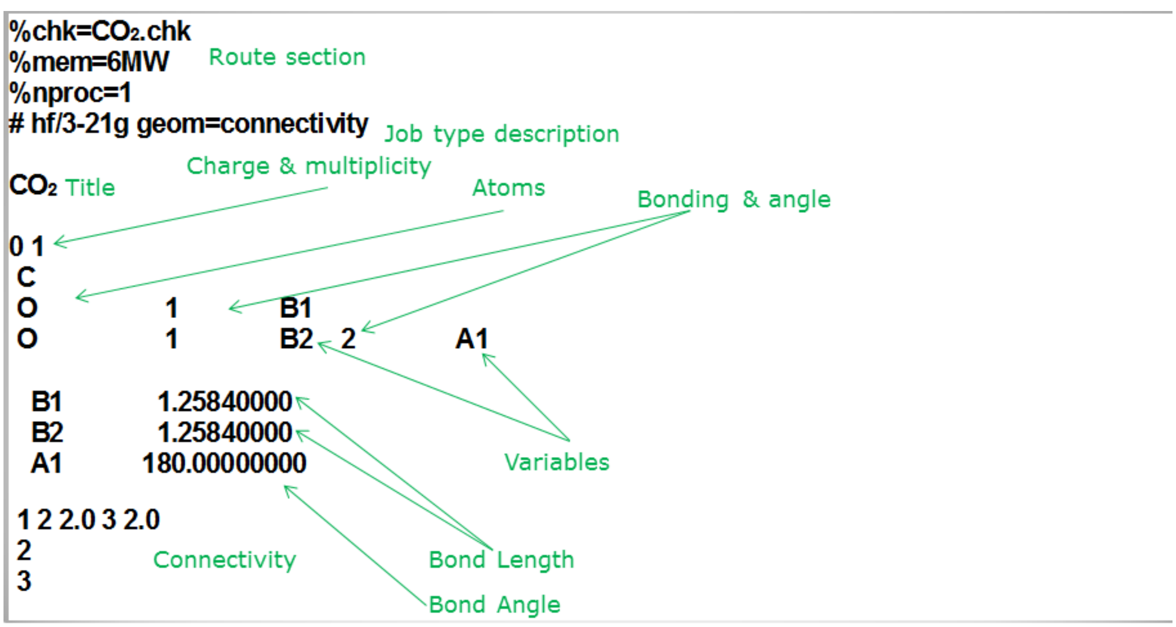

Figure 3. Gaussian 03 input file

The checkpoint file records all of the calculations made by the program for use with different jobs being run on the same molecule (optimization and energy). This section is also where the computer usage was specified. The number of processors and the amount of memory used was specified based on the advice of the PSC. The major advantage of using the PSC is that the researcher is given access to a multiplicity of computers. Once the researcher has the skill to use Gaussian 03, supercomputing resources and to unify the two it is possible to make much more efficient use of computational time by uploading multiple jobs onto different resources at once. The effectiveness of the supercomputing software after some level of mastery was achieved counteracted the disadvantage of spending so much time waiting for the outputs (6-10 hours). Uploading only one at a time would limit the researcher to run one job per day and two if there were smaller compounds (ring cleavage metabolites). The job type description specifies the theory and the basis sets but can also specify special details to calculate different things or to limit how the calculations will change the molecule during optimization. The charge-multiplicity section specifies the charge of the molecule and the spin multiplicity (singlet or triplet) allowed within orbitals. The next sections involve the specific molecular composition. The connectivity is a special section using the special keyword GEOM to ensure that the molecule is not changed during optimization.

After the optimization and energy calculations have been completed the output files are analyzed the electron density can be calculated. The highest occupied molecular orbitals (HOMO) are identified and the energy of those orbitals is used to calculate the frontier electron density. These orbitals are used when electrophilic reactions occur. The LUMO orbitals are used when nucleophilic reactions are of interest and both are used when radical transformations take place. The following equation is used with the energy of the HOMO orbitals to calculate the FED.

$$f_r = \sum 2 * C_{fr}^{\ 2}$$

Figure 4. FED equation

In this equation C_{fr} represents the energy of the HOMO and f_r is the electron density of the given electron. FED is calculated for each carbon atom. The FED of EE_2 and a number of metabolites were calculated using both theories and basis sets but all molecules were calculated using DFT/6-31g(d) basis set.

A comparison of the basis sets STO-3G and 6-31G(D) and theory were carried out to determine the viability of the lesser methods in favor of computational costs time wise. The first comparison was between the two different basis sets. The first calculations were done using the STO-3G basis set with the HF theory. These calculations represent the lowest level of calculation. Consequently, these calculations also took the least amount of time. The second set of calculations involved calculating the electron density using a much higher and more accurate split valence basis set; 6-31G(D). The third set of calculations compared the two theories; HF and DFT at the higher basis set after the comparison of the first two basis sets. After all comparisons were complete FED profiles were generated for all experimentally measured and predicted metabolites and sorted into metabolic pathways starting from EE_2 and when possible, extending to the first ring cleavage.

2.3 DEGRADATION RULES

After determining high probability reaction sites, degradation rules based on the work of several separate research groups were applied to produce metabolic pathways leading up to ring cleavage. The following 6 rules have been applied to the FED calculations. (Kamath and Vaidyanathan1990; Hay and Focht 1998; Nosova et al. 1997; Nagy and Fabian 2006; Stephan et al. 1997; Casellas et al. 1997; Dean-Ross et al. 2001; Brzostowicz et al. 2005; Nakazawa and Hayashi and Hayashi 1978; Olsen et al. 1994)

Rule 1 – The enzyme attacks the carbon atom at the highest FED. The carbon atom being oxidized must be bound to a –H, =O, or –OH group.

Rule 2 - The phenol ring is cleaved after being oxidized to catechol. Oxygenolytic cleavage of the phenol ring occurs via Ortho- or meta-cleavage. Ring cleavage takes place between the hydroxylated carbon with highest FED value and carbon with higher FED out of two adjacent carbons.

Rule 3 – The cyclohexane and cyclopentane rings are opened after oxidation to cyclohexanone and cyclopentanone, respectively. Ring cleavage of either cylcohexanone or cyclopentanone is determined by the same rule with phenol ring cleavage.

Rule 4 - After ring cleavage, carbon chains are degraded to hydroxyl-, ketone, and carboxylic acid, followed by a de-carboxylation step.

Rule 5 – Resonance can cause the phenol ring to be converted to a semiquinone tautomer, which can be oxidized according to degradation rules 1-4.

Rule 6 – If the degradation rules are not applicable to rules 1 through 4, enzymatic attack proceeds at the carbon atom with the second highest FED value.

Figure 5 illustrates degradation rules 2-5.

Rule 2:

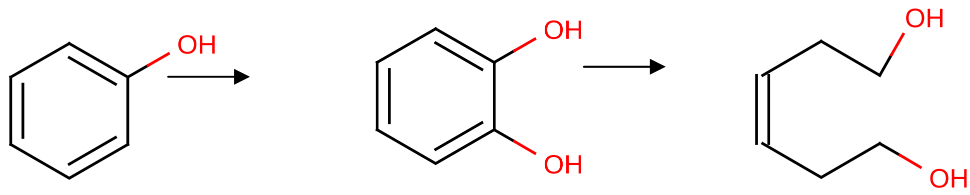

Rule 3:

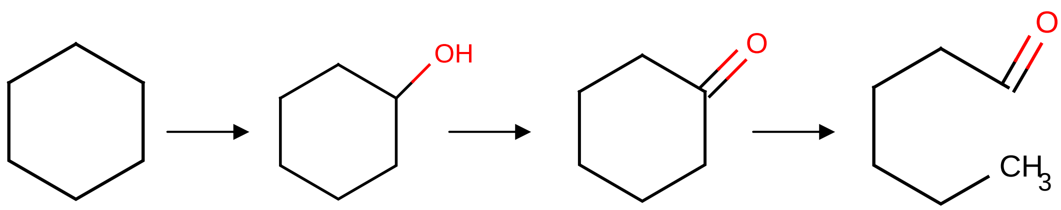

Rule 4:

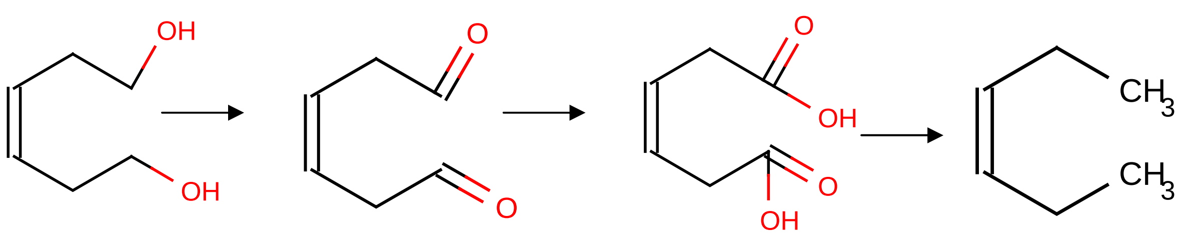

Rule 5:

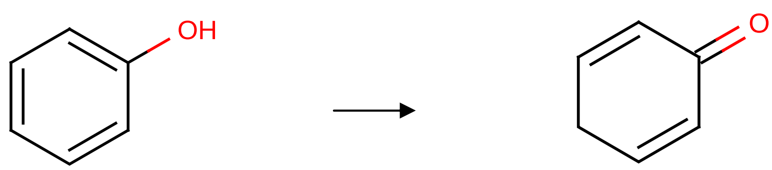

Figure 5. Degradation Rules

2.4 ESTROGENIC POTENTIAL

The three factors for determining estrogenic potential are n_a, n_d, and hydrophobicity. The number of donor groups is calculated based on the number of hydrogens attached to atoms capable of participating in hydrogen bonding. In this study, only oxygen was capable of forming hydrogen bonds and each functional group was counted as one. For hydrogen bond acceptors, in a fashion similar to Lipinski et al. (2001) all oxygen atoms (no nitrogen is present) were counted as n_a. The method for calculating the hydrophobicity was an additive approach that assigns each atom a value based on the surrounding bonds. Figure 6 shows an example of how logP is calculated using this additive method (Viswanadhan et al., 1989). This method has been validated using experimental results for a number of different molecules to determine the octanol-water coefficient. This calculation was done using the free online chemaxon software (2009). The blue values are positive hydrophobicity, the red are negative and the grey is neutral.

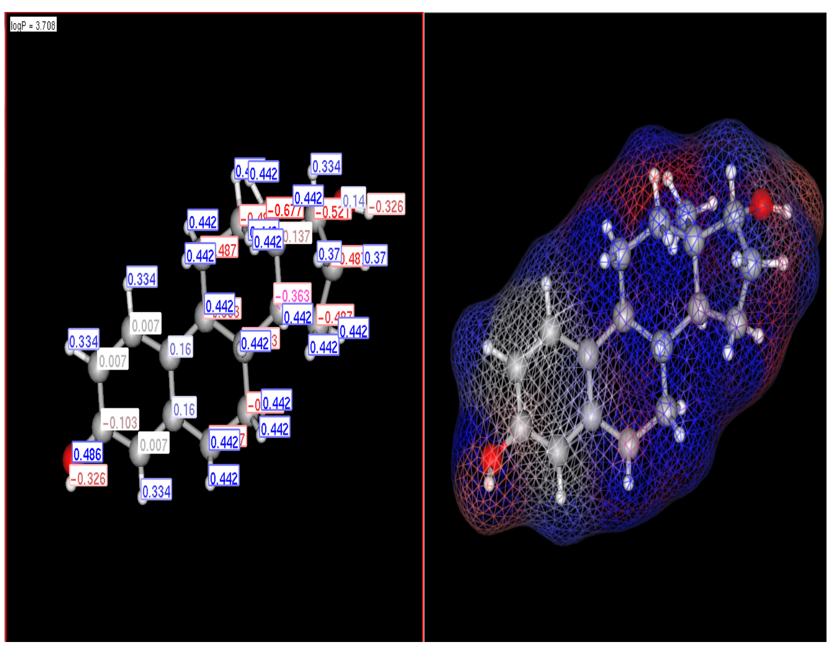

Figure 6. Hydrophobicity of E_2

3.0 RESULTS

3.1 FRONTIER ELECTRON DENSITY

The frontier electron density of EE_2 was calculated using all basis sets and theories. In order to relate the carbon site numbers in charts containing FED data to the actual structure the standard numbering procedure was applied to the figure as presented in Gaussian 03. Figure 7 shows EE_2 with the atoms numbered.

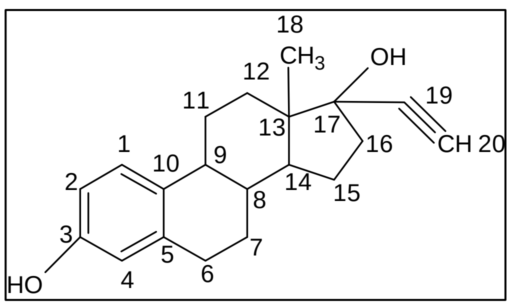

Figure 7. EE_2 with atom labels

These labels will be used for all of the steroidal estrogens and metabolites. The rings shall be referred to by letters starting from the left going right letters A through D. After each carbon is assigned a number it is possible to get a better look at the electron density profile for EE_2. Figure 8 shows the electron density profile of EE_2 using DFT. Referring to both figure 7 and 8 the first thing that is apparent is that the highest reactive sites are in Ring A.

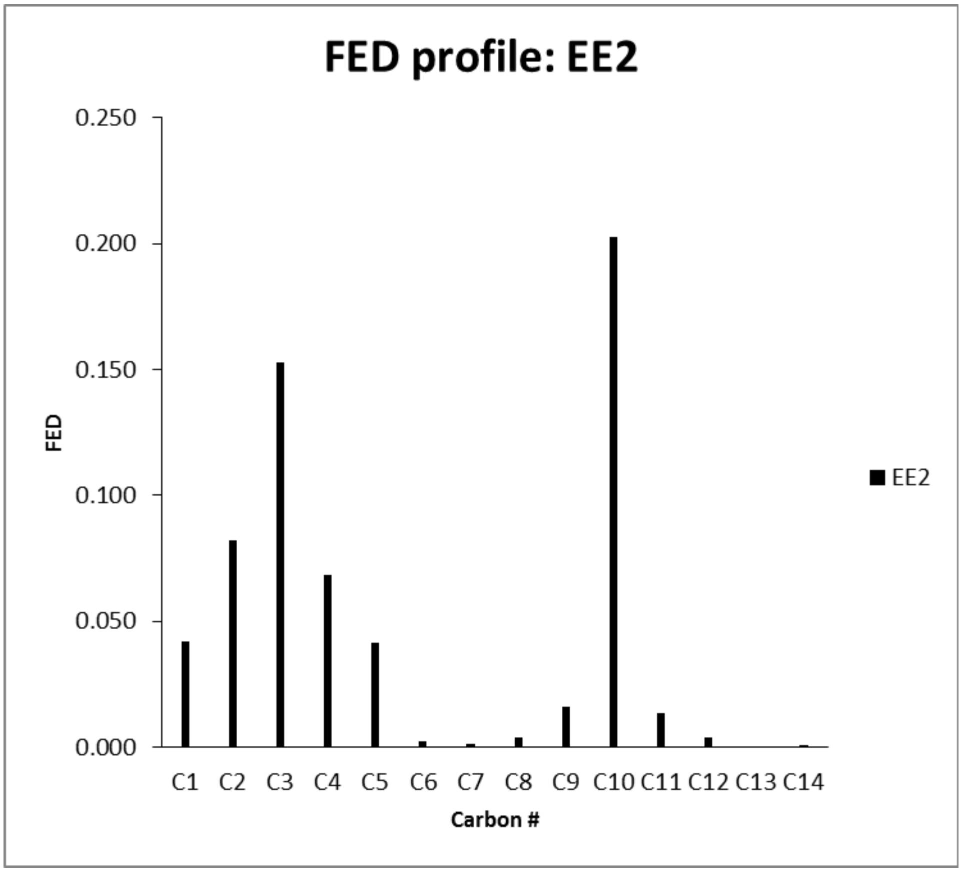

Figure 8. EE_2 FED at each carbon site

The carbon sites with relevant electron density are carbons 1, 2, 3, 4, 5 and 10 which are the six carbons that make the phenolic ring. This is consistent with the two studies mentioned earlier (Yi 2007 and Khunjar 2011) with metabolites detected with ring A cleavage.

3.2 INITIATING REACTIONS

Figure 9 illustrates the three metabolites that have been published in literature based on experiments for investigating the biodegradation of EE_2. Initiating reactions occur at carbon units with high electron density.

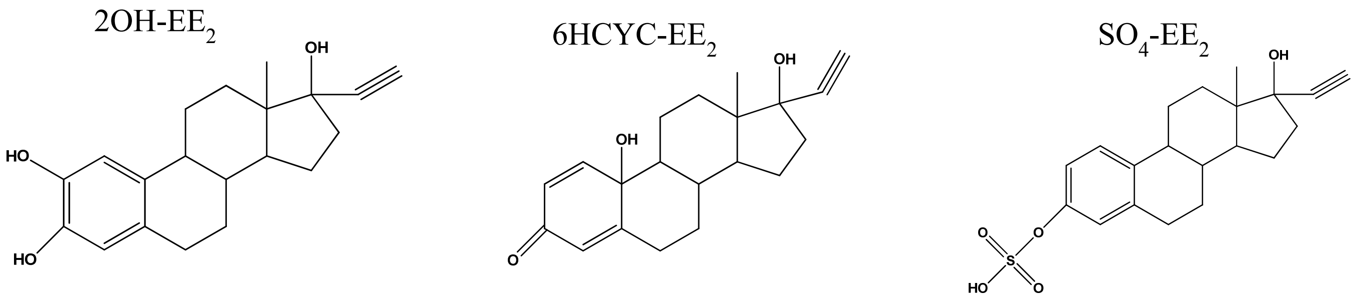

Figure 9. Initiating metabolites

Each of these reactions occurs at one of the highest three electron density sites. In the case of 2OH-EE_2, hydroxylation at the C2 carbon site is the initiating reaction. This is the third highest electron density site and the highest site where an addition reaction is possible without any transformation to the phenolic ring. This is the type of transformation that would generally be expected to occur on a phenolic ring. This oxidation is an electrophilic substitution at the ortho position which plays a role in further biodegradation based on the rules established for this study. The second metabolite, 6HCYC-EE_2 is a transformation at the C10 carbon that occurs after tautomerization of ring A. Prior to this process, it is impossible for a hydroxylation to occur at the C10 carbon. The third transformation is actually a conjugation from a hydroxyl group to a sulfate functional group in its place. The third carbon is the second highest electron density position. The detection of these three initial metabolites is consistent with FED-based theory.

The electron density profiles for the three initial metabolites were also calculated. These charts were to illustrate the effect of each biological transformation on the electron density. Each transformation only involves one step and so it is expected that the change in electron density should only take place at or near the carbon site where the biotransformation takes place. Figure 10 compares the electron density of EE_2 to 2OH-EE_2. The electrophilic reaction occurs at C2.

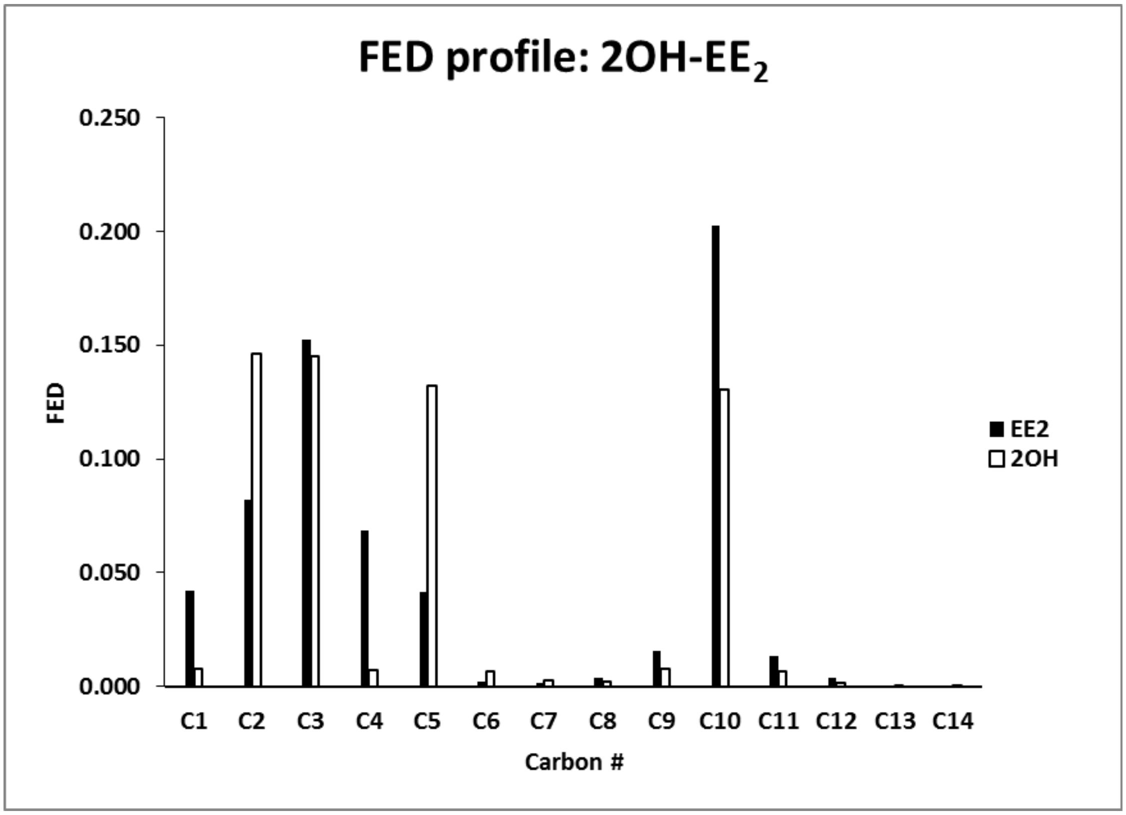

Figure 10. 2OH-EE_2 compared to EE_2 based on the initial transformation

The profile of 2OH-EE_2 is interesting because of the increase of electron density at that location. The electrophilic attack should draw electrons away from that location, because of the higher electronegativity of the hydroxyl group in comparison to the carbon atom, but that is not the case. This has been attributed to the phenomenon redox induced electron rearrangement (RIER). RIER asserts that upon oxidation the removal of an electron causes local orbitals to relax which leads to a reconfiguration of the electron density that results in an increase in the electron density. Figure 11 illustrates the electron density profile for 6HCYC-EE_2. This is the only transformation at the highest FED value of the parent compound but unlike the other two byproducts the shifting of electrons occurs in multiple locations.

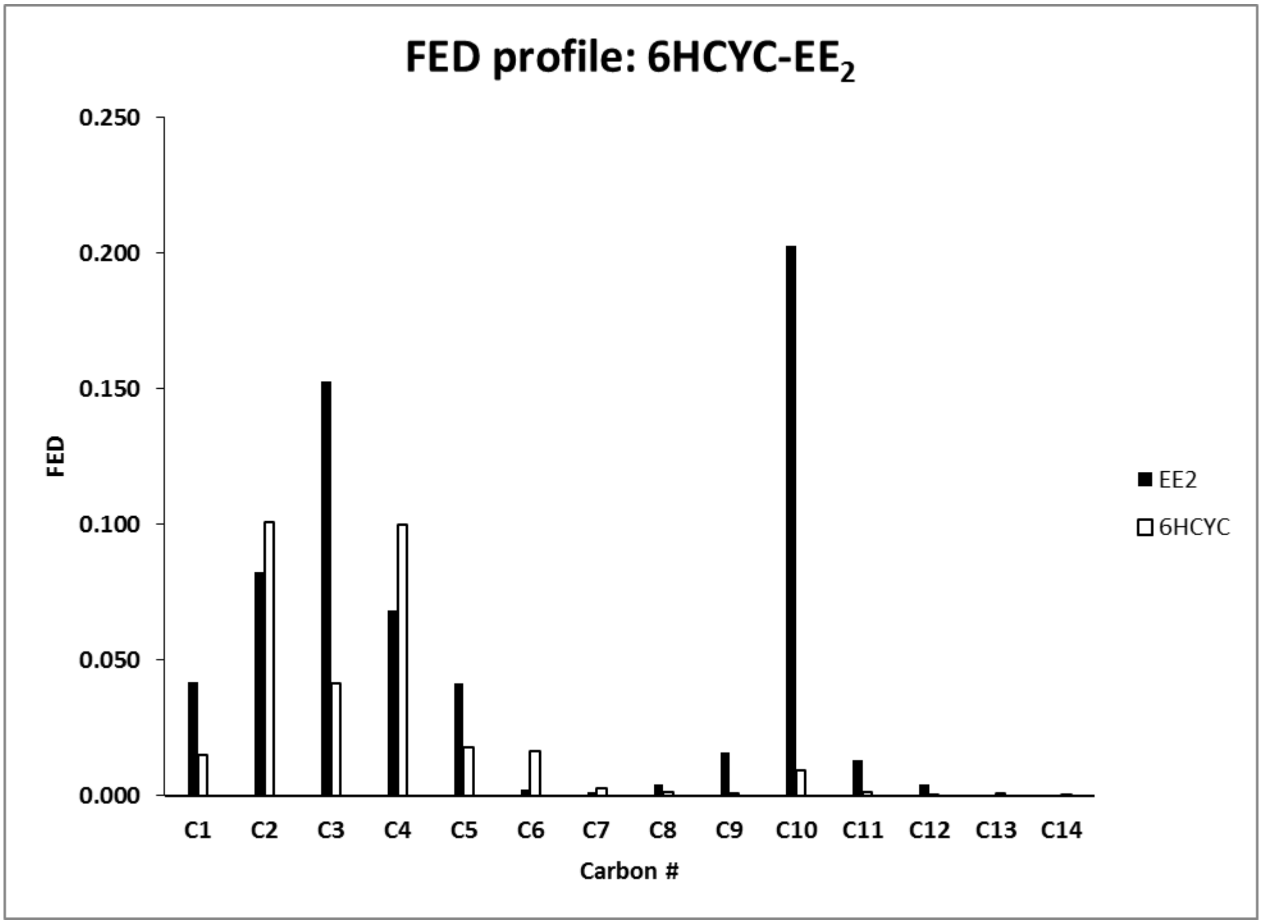

Figure 11. 6HCYC-EE_2 FED compared to the parent compound

This pathway shows a dramatic decrease in the total electron density of the molecule. The electron density has decreased by over 50% from EE_2 to 6HCYC-EE_2 (0.631 to 0.309). This result is not surprising because ring A is no longer aromatic and has lost much of its reactivity and stability. Also the oxidation at C10 removes nearly all of the electron density unlike the first pathway. Figure 12 shows the FED profile for SO_4-EE_2 and EE_2.

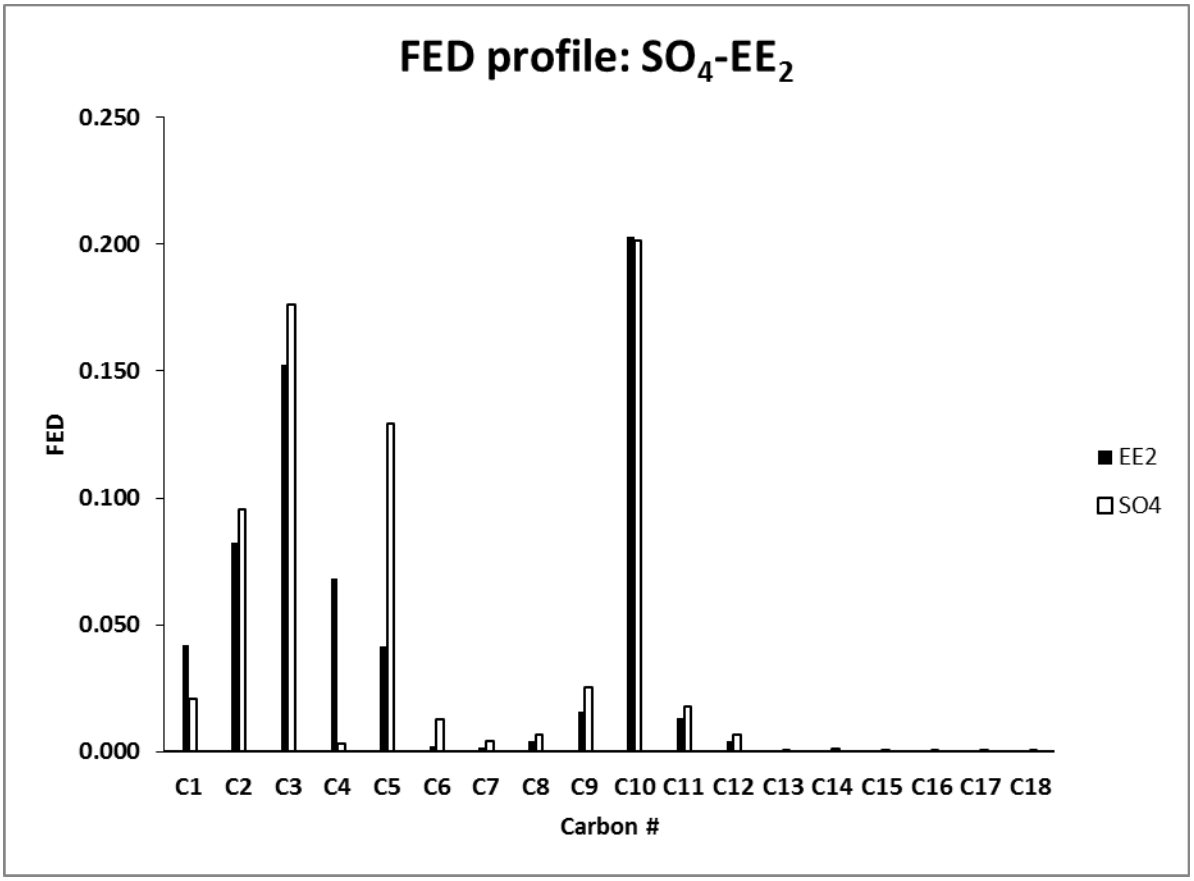

Figure 12. SO_4-EE_2 FED compared to the parent compound

Sulfo-EE_2 appears to be recalcitrant. Khunjar et al., 2011, recently found that Sulfo-EE_2 was not degraded by heterotrophic cultures that were otherwise active. Further, I hypothesize based on the increase in the size of the functional group, that steric interferences cause sulfo-EE_2 to be significantly less reactive than the other initiating metabolites. C3 contains the much larger sulfate group (compared to hydroxyl) which may interfere with the reactivity of both adjacent carbons (C2 and C4). Despite the increase in electron density the presence of the sulfate group may end up being responsible for limiting the reactivity of this metabolite. C10 and C5, which make up the majority of the electron density, are also unavailable for addition reactions for reasons stated during the discussion of 6HCYC-EE_2

3.3 THEORY AND BASIS SET COMPARISON

After successfully completing Gaussian 03 jobs, HF theory was applied to both basis sets and results were compared. In all cases for geometric optimization the lower basis set was faster than the higher basis set by a number of hours (data not shown). Figure 13 shows a comparison of the two basis sets when implemented with HF theory.

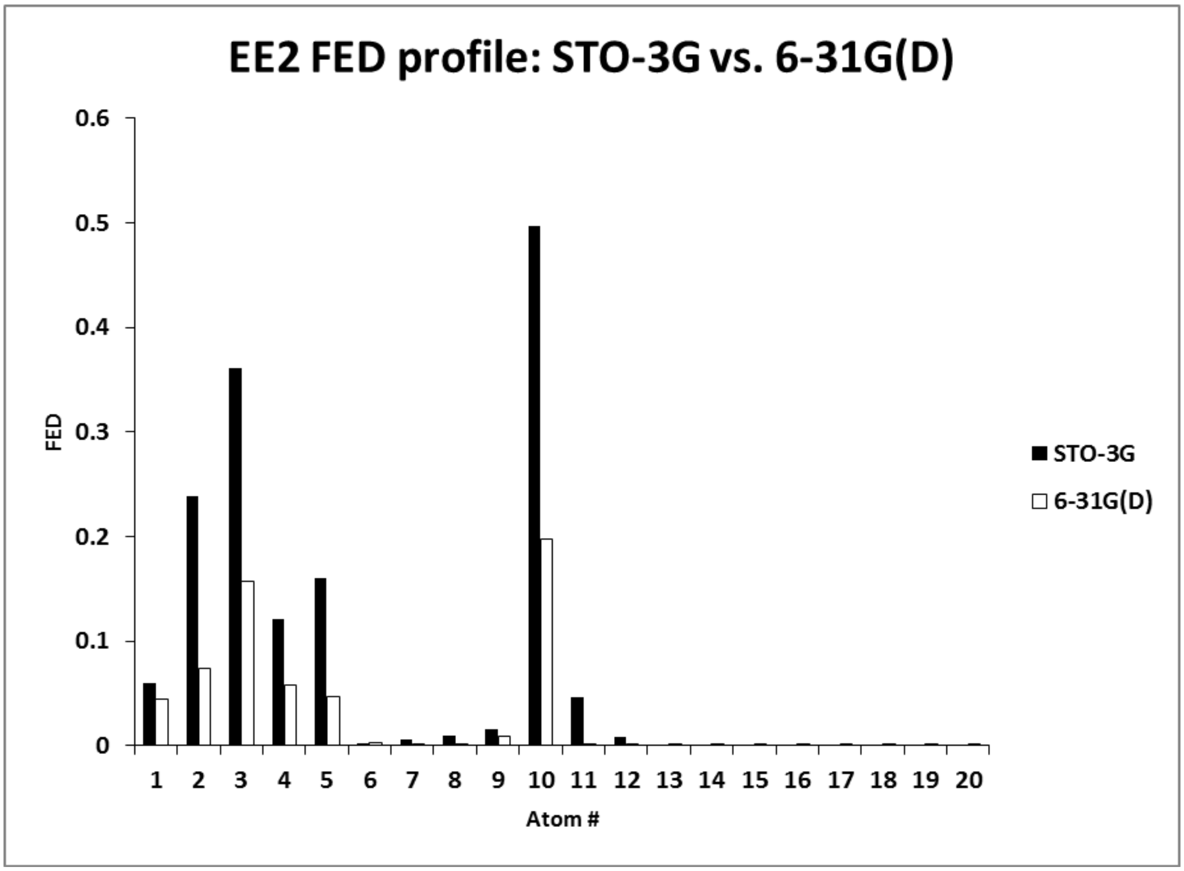

Figure 13. Electron density comparison of basis sets STO-3G vs. 6-31G(D)

Figure 13 shows the electron density calculation for EE_2 using two different basis set. Ideally, these profiles should be identical. The magnitude of the difference at each carbon site illustrates the need to employ the better basis set if feasible. The comparison of the FED profile for EE_2 shows that the lower basis set over-estimates the electron density at all relevant carbon sites (C2, C3, C4, C5 and C10). The largest difference is 0.29 for C10. The lower basis set FED value was more than double the value at the higher basis set. This result is within expectations because the first step of the process is an optimization to the lowest energy conformation. The lower STO-3G basis set uses less rigor and so the lowest energy conformation it is capable of calculating is not as low as the conformation calculated by the higher basis set. The lower basis set does however show the same high electron density sites (and carbon site higher than 0.1) as the higher basis set. In the case of both basis sets the highest three reactive sites follow the same trend (C10>C3>C2). The difference in the accuracy can be further illustrated by the time it takes to run Gaussian 03 jobs using both basis sets. The lower basis set takes approximately one hour to complete. The split valence basis set takes between 6 and 10 hours. This data indicates that the limiting factor in using the Gaussian 03 software is the basis set being applied. Given that the more accurate basis set was available without too much of a difference in computational time, (~9 hour difference between them in the worst case), the higher basis set was used for developing transformation pathways.

HF and DFT show similar FED profiles for EE_2. DFT is slightly higher than HF at all relevant carbon sites (FED>0.05). The two theories also predict the same reactive carbon sites and nearly identical absolute electron densities. The largest difference between the two theories in this case occurred at C2 and was 0.01652. In most cases using DFT required more time than HF (~8 or 9 hours). However, the highest calculation time was for HF using SO_4-EE_2. (~10 hours) This work shows that the basis set selected has a much greater effect on the FED calculation than the level of theory. The basis set affects the time and the calculated energy eigenfunctions. The theory plays a much less significant role in calculation. This is not entirely surprising as both theories define molecular orbitals in similar fashion and require the same solution method as defined by Fock. For consistency, the rest of the FED results figures were calculated using DFT as the more advanced theory. Other comparisons are presented in the Appendix.

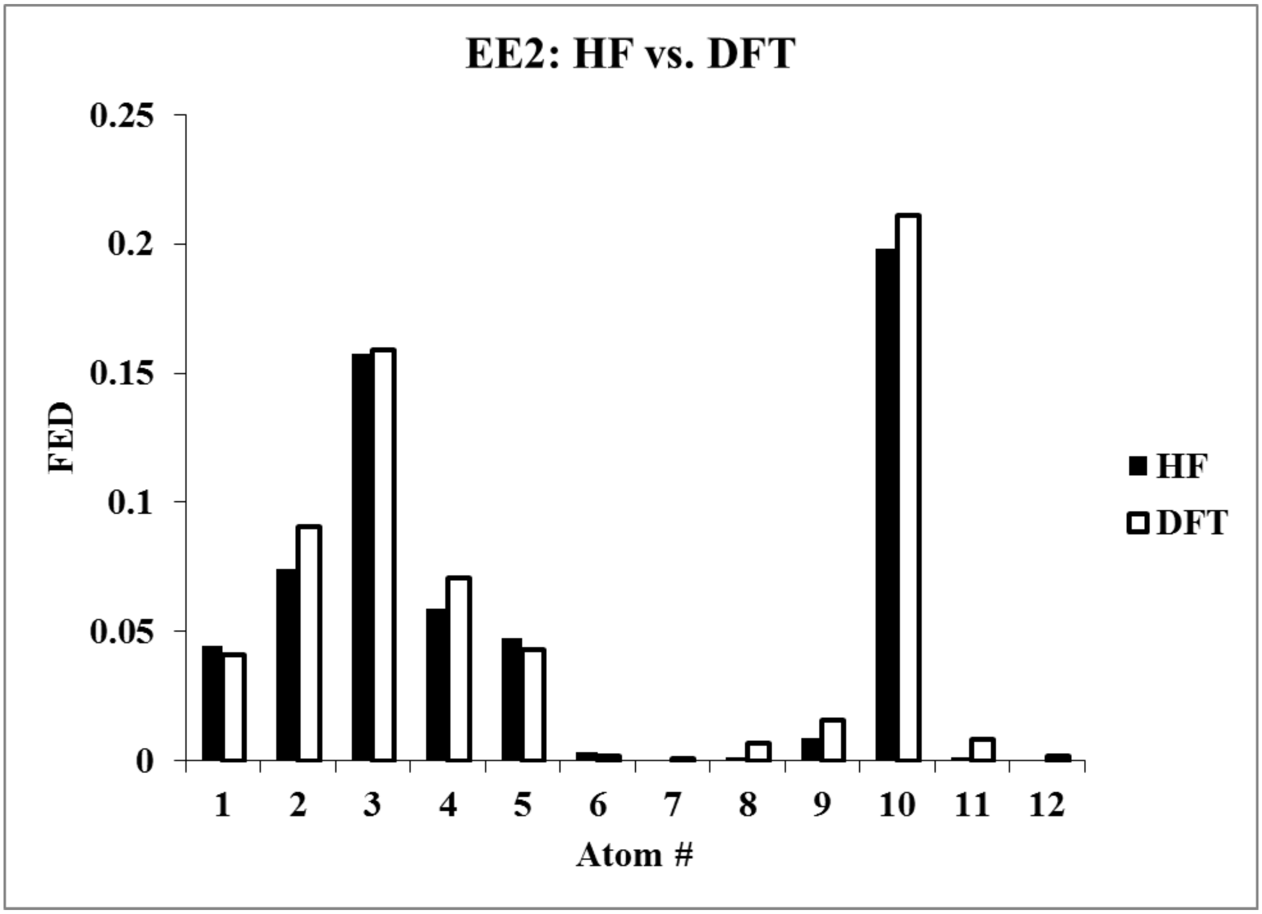

Figure 14. Theory comparison HF vs. DFT

In deciding which method to use for the duration of the study the calculation times were examined as well as the accuracy based on a review of the literature (refer to methods section) Table 1 gives the results of the comparison between the two basis sets. This table was used to compare the pros and the cons of the basis sets to determine which one should have been used or if either one would have been acceptable.

Table 1. Analysis of Basis Sets

	STO-3G	6-31G(D)
Pros	-Very short run time -Highest sites correctly predicted	-Noticeably better definitions of molecular orbitals -Time disadvantage alleviated by using PSC
Cons	-all FED values are severely overestimated	-Takes 6 to 10 hours per job

Based on the results presented in Figure 13 and the analysis done in Table 1 it was necessary to employ the higher basis set to confidently present quantitative results. Table 2 compares the two theories based on Figure 14 and other theory comparisons that have been performed.

Table 2. Analysis of Level of Theory

	HF	DFT
Pros	-Slightly shorter run times usually -Highest sites correctly predicted -Differences to DFT are almost negligible	-Better definition of molecular orbitals -sometimes shorter than HF
Cons	-Theoretically not as accurate as DFT -Not always shorter -Takes 6-10 hours per job	-8-9 hours per job

The two theories showed very similar FED trends and either could have been used. HF could have been used if it always proved to have a shorter runtime than DFT. In most cases HF was shorter than DFT, but for sulfo-EE_2, the HF runtime was longer than the DFT runtime. DFT and HF had similar run times in most cases making time a much smaller issue in this study, therefore DFT was selected because it is the more rigorous theory. Appendix 4 contains additional figures comparing the basis sets and the theories.

3.4 PATHWAYS

Figure 15 illustrates the pathway that was generated, starting with the initiating reaction that produces 2OH-EE_2.

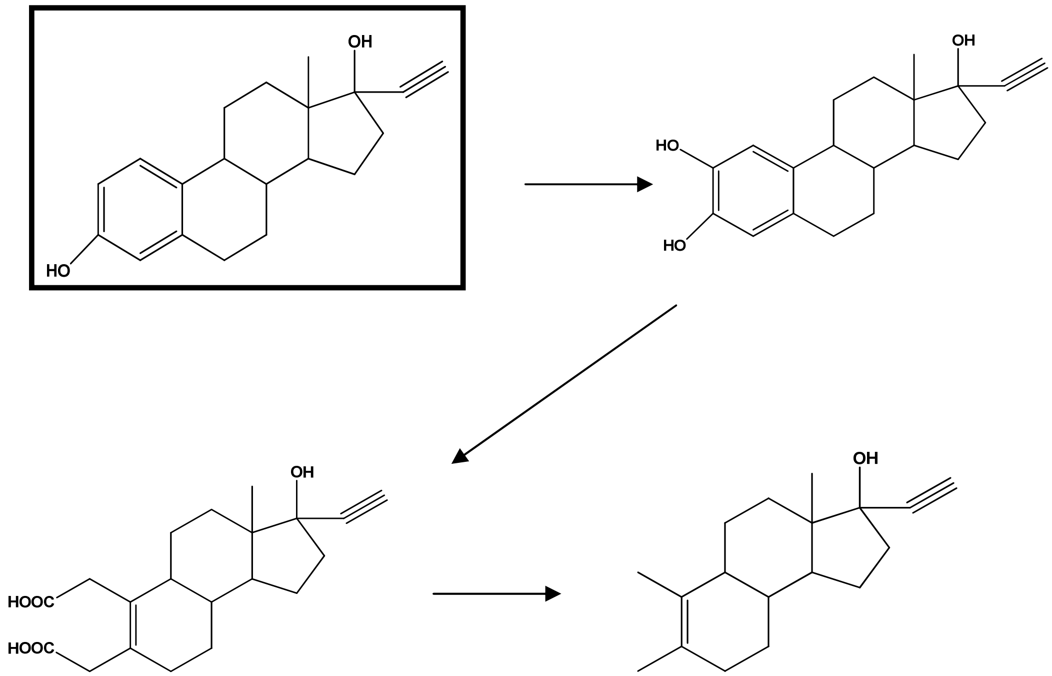

Figure 15. 2OH-EE_2 pathway

After the hydroxylation of EE_2 at the C2 carbon site 2OH-EE_2 is produced. This molecule contains a catechol molecule in the first ring. The next step is ring A cleavage, followed by the degradation of the hydroxyl groups to carboxylic acid groups. The final metabolite in this pathway is ETDC, which occurs after decarboxylation, and has been detected by Yi and Harper, 2007. The existence of this pathway shows the capabilities of the coupled FED theory and degradation rules not only to predict initiating reactions but also ring cleavage metabolites. The second pathway is represented in Figure 16 and starts with the tautomerization, which removes one of the double bonds out of the ring to form the ketone group in place of the hydroxyl group.

This transformation exposes the highest FED position for oxidation. The second transformation step produces 6HCYC-EE_2, which was detected in the effluent of a microalgae-based bioreactor (Della-Greca et al. 2008). The next step is an ortho-transformation which leads to the third metabolite, also similar to a catechol molecule with one of the hydroxyl groups changed to a ketone group prior to ring cleavage. This is followed by ring cleavage and then transformation of the hydroxyl and ketone functional group to carboxylic acid groups. The final metabolite shows the decarboxylation step.

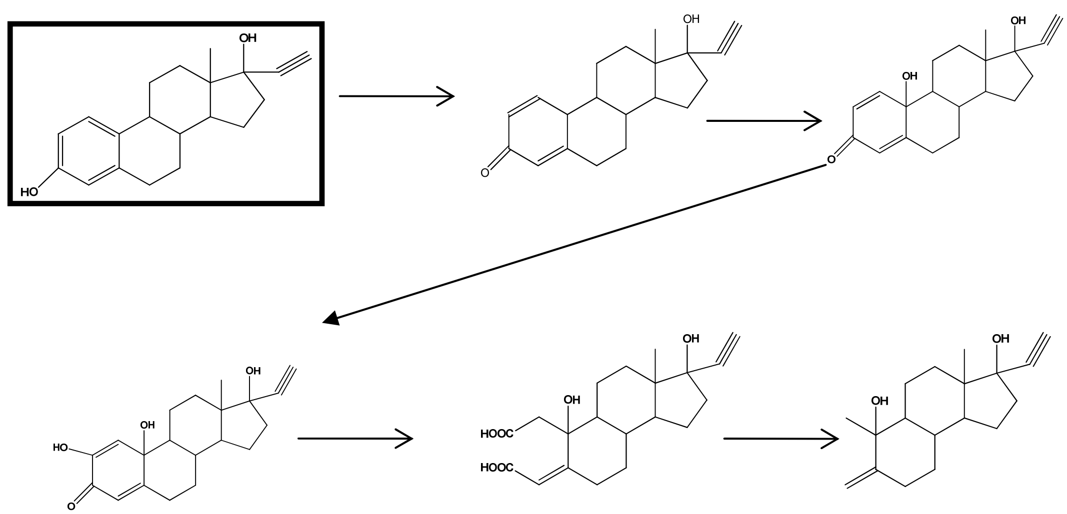

Figure 16. 6HCYC-EE_2 pathway

Prior to tautomerization, the C10 carbon is already single bound to two carbons and double bound to a third. This makes it impossible for any type of addition reaction to take place at the C10 carbon. This is a critical pathway for two reasons. It is the only pathway with a transformation occurring at the highest electron density and it is the only pathway where ring A has its aromaticity removed. For the final metabolite, SO_4-EE_2 there is no pathway. This is significant because while it has been detected in activated sludge it also exists in other areas.

Specifically fish are known to conjugate EE_2 into SO_4-EE_2 to detoxify and make SO_4-EE_2 easier to excrete (Kotov 1999; Zamek-Gliszczynski 2006). This is an important factor not only in terms of reactivity but also toxicity. Khunjar et al. (2011) detected sulfo-EE_2 as well but did not detect any further degradation while using a nitrifying culture followed by a heterotrophic culture in series. Hutchins et al. (2007) indicated that sulfatase enzymes were capable of deconjugating SO_4-EE_2 but the only conjugates they were able to detect above 1 ng/L were sulfate conjugates. This is consistent with our results showing sulfo-EE_2 being recalcitrant. SO_4-EE_2 also does not fit within the established degradation rules of this study. Sulfo-EE_2 may either be a "dead-end" metabolite, or it may be transformable after desulfurization, which may be a slow process (Hutchins et al. 2007). Wastewater treatment plants that are interested in EE_2 should look for Sulfo-EE_2 in secondary effluent.

3.5 ESTROGENIC POTENTIAL

The estrogenic potential of the pathways and metabolites presented in the previous sections was analyzed based on the factors indicated in literature using structural analysis relationships. This data does not quantify estrogenic potential but estimates the direction and magnitude of the change qualitatively based on those key factors that are calculated. Table 3 illustrates the change of estrogenic potential for EE_2 and each metabolic pathway. The most important factor to consider was the hydrogen bond donor groups followed by the acceptor groups that are capable of competing with the estrogen receptor. The hydrophobicity was the lowest impact factor because it involves the entire ligand and receptor while the other two factors focus only on the active sites. Based on the estrogenic potential rules discussed previously, EHMD is predicted to have a lower estrogenic potential than EE_2because the n_a is greater (3 vs. 2), the n_d is unchanged, and the log P is smaller than that of EE_2 (2 vs. 3.7). Sulfo-EE_2 also appears to have lower estrogenic potential than EE_2 for similar reasons. OH-EE_2has a lower log P (3.4 vs. 3.7) and higher n_a (3 vs. 2) compared to EE_2, but it also has an additional hydrogen bond donating group, a fact that may counterbalance the changes in log P and n_a.

Table 3. Estrogenic Potential analysis for metabolic pathways

Pathway	Compound	H-bond donors	H-bond acceptors	logP	Change in estrogenic potential
2OH-EE_2	EE_2	2	2	3.72	
	2OH- EE_2	3	3	3.43	**Slight Decrease**
	EDMC	3	5	1.48	**Decrease**
	ETDC	1	1	3.77	**Decrease**
6HCYC-EE_2	EHMD	1	2	3.19	**Decrease**
	6HCYC-EE_2	2	3	2.02	**Decrease**
	ETMD	3	4	1.11	**Decrease**
	CEDM	4	6	0.82	**Decrease**
	EDMC	2	2	1.99	**Decrease**
SO_4-EE_2	SO_4-EE_2	2	5	2.96	**Decrease**

Thus, in this case the change in relative estrogenic potential is not as clear, however, we hypothesize that 2OH-EE_2 has less estrogenic potential than EE_2 because previous work has shown that 2OH-E_2 (not 2OH-EE_2) is less estrogenic than E_2. If hydroxylation at C2 reduces estrogenicity for E_2, it seems reasonable to expect the same for EE_2 (Lee 2008).

Estrogenic potential changes during the course of the transformation pathways. For example, during the EE_2-to-EDMC pathway (Figure 15), there are clear indications that estrogenic potential decreases during the steps leading to ring cleavage; the log P decreases and the n_a increases. The last compound in the pathway (EDMC) is without the active phenolic ring, and is therefore likely to have lower estrogenic potential. There are, however, two predicted metabolites (i.e. ETMD and CEDM) that have a higher n_d (3 and 4 respectively) than EE_2. These two compounds should probably be tested for estrogenicity in future efforts. During the EE_2-ETDC pathway, there are also indications that estrogenic potential is reduced (Figure 16). OH-EE_2 (as mentioned earlier) is likely less estrogenic than EE_2, and EMDC has less estrogenic potential than OH-EE_2 (or EE_2) because it has lower log P and higher n_a. The last compound in this pathway (ETDC) has lost the active ring and likely has lower estrogenic potential than EE_2. Finally, it has been shown that Sulfo-EE_2 has less estrogenicity than EE_2 (Kotov 1999; Buikema 1979). We hypothesize this based on previous studies that have linked hydrogen bonding and hydrophobicity to receptor activity (Lipinski, 2001) because Sulfo-EE_2 has a lower log P than EE_2 (i.e. $3.0<3.7$, Figure 17) and Sulfo-EE_2 has a higher n_a ($5>2$, Figure 17). The higher number of acceptors limits the probability that the remaining hydrogen bond donor group will interact with the ERE. Sulfate conjugation does not change n_d.

4.0 CONCLUSION

FED theory was used to successfully predict the initiating reactions for EE_2 transformation. One reaction showed an oxidation at the highest available non-substituted carbon site. The second reaction modified ring A to make it susceptible to an electrophilic attack at the highest FED value of EE_2 after the occurrence of tautomerization; a process rarely seen in biological removal of EE_2. The third reaction showed the sulfate conjugation of the 3-hydroxyl group attached to the second highest FED position to occur in activated sludge. The occurrence of these reactions at high electron density indicates that frontier electrons play a pivotal role in biological transformations of EE_2.

The use of Gaussian 03 with the PSC made it possible to explore more than one method of calculating the electron density. The basis sets were shown to have a dramatic effect on the calculation procedure in terms of time and accuracy. Access to the PSC allowed for the implementation of the higher basis set that would not have been possible with an individual personal computer. HF and DFT showed similar performance in determining electron density. HF uses a broad account of electron-electron interactions by using a central field approximation. This approximation gives an electron-electron correlation embedded within the solution to the wave function that represents the electron. The electron density calculated by DFT shows higher results than those calculated by HF theory but the order of highest electron density sites is consistent between the two theories. DFT is more accurate for calculating electron density but

HF theory is still viable for judging the order of the reactive sites when calculating the electron density for EE_2.

Determining which ring is cleaved first is a critical step in analyzing the detoxification of EE_2. All initiating reactions occurred on ring A in this study. Application of the degradation rules to the initial metabolites led to two instances of ring A cleavage metabolites and one dead end pathway. The existence of the first ring A cleavage metabolite; ETDC indicates that ring A is the first ring cleaved in biological transformations and the use of the degradation rules and FED further reinforce this supposition.

All pathways showed a decrease in estrogenic potential but some of that potential may be retained. The importance of the steroidal estrogens has been a critical concern in the environmental community for years. This use of methods capable of predicting the reactivity of such potent EDCs as well as their toxic nature is a novel method in analysis without the use of expensive and difficult experimental techniques. With supercomputing resource and brief, readily available training, companies can better predict the fate of their products and active ingredients prior to fully marketing a product. This step is neither difficult nor costly and should be considered as a logical step for any company preparing to release a product that will have significantly affect bodily functions and potentially reach unintended consumers via recalcitrant toxicants further burdening wastewater treatment. FED theory by no means replaces experiment, but can rather provide a map of what researchers should be looking for when attempting to identify EDCs in trace amounts and quantify their toxic effects.

APPENDIX A

GAUSSIAN INPUT FILES

The following file contains the molecular specification of E_1 as an example of what a Gaussian 03 input file looks like. Refer to Figure 3 for an explanation of each section when CO_2 was used as the input file.

```
%chk=1.chk
%mem=6MW
%nprocs=1
# ub3lyp/6-31g(d) guess=(read,only) geom=connectivity

1

0 1
 C
 C    1   B1
 C    2   B2    1   A1
 C    3   B3    2   A2    1   D1
 C    4   B4    3   A3    2   D2
 C    1   B5    2   A4    3   D3
 C    6   B6    1   A5    2   D4
 C    5   B7    4   A6    3   D5
 C    8   B8    5   A7    4   D6
 C    9   B9    8   A8    5   D7
 C    7   B10   6   A9    1   D8
 C   11   B11   7   A10   6   D9
 C   10   B12   9   A11   8   D10
 C   11   B13   7   A12   6   D11
 C   14   B14  11   A13   7   D12
 C   13   B15  10   A14   9   D13
 C   15   B16  14   A15  11   D14
 O   15   B17  14   A16  11   D15
```

O	3	B18	2	A17	1	D16
C	14	B19	11	A18	7	D17
H	1	B20	2	A19	3	D18
H	2	B21	1	A20	6	D19
H	4	B22	3	A21	2	D20
H	7	B23	6	A22	1	D21
H	8	B24	5	A23	4	D22
H	8	B25	5	A24	4	D23
H	9	B26	8	A25	5	D24
H	9	B27	8	A26	5	D25
H	10	B28	9	A27	8	D26
H	11	B29	7	A28	6	D27
H	11	B30	7	A29	6	D28
H	12	B31	11	A30	7	D29
H	12	B32	11	A31	7	D30
H	13	B33	10	A32	9	D31
H	16	B34	13	A33	10	D32
H	16	B35	13	A34	10	D33
H	17	B36	15	A35	14	D34
H	17	B37	15	A36	14	D35
H	19	B38	3	A37	2	D36
H	20	B39	14	A38	11	D37
H	20	B40	14	A39	11	D38
H	20	B41	14	A40	11	D39

B1	1.39203384
B2	1.39758486
B3	1.39400685
B4	1.39842832
B5	1.40222384
B6	1.52834980
B7	1.51749145
B8	1.52994854
B9	1.53274874
B10	2.58876945
B11	1.54416233
B12	1.54527743
B13	1.54417836
B14	1.54335444
B15	1.55506537
B16	1.52493284
B17	1.21300836
B18	1.36885561
B19	1.54237918
B20	1.08606621
B21	1.08808657

B22	1.08627572
B23	1.10156336
B24	1.10000574
B25	1.09617596
B26	1.09628652
B27	1.09909057
B28	1.10168795
B29	1.09723546
B30	1.09451617
B31	1.09532745
B32	1.09561053
B33	1.09967193
B34	1.09333123
B35	1.09744697
B36	1.09270933
B37	1.09974400
B38	0.96605039
B39	1.09579107
B40	1.09411194
B41	1.09335041
A1	119.35064534
A2	119.45169162
A3	121.12422670
A4	122.16112515
A5	119.90793401
A6	118.78402358
A7	112.69771662
A8	110.57682001
A9	141.01188262
A10	33.55463788
A11	112.57362234
A12	84.28985868
A13	109.49844419
A14	112.98986547
A15	109.63635616
A16	124.38301406
A17	122.88446608
A18	111.08707082
A19	118.36672634
A20	120.27965650
A21	118.49912810
A22	106.58267508
A23	109.00138233
A24	109.52216912
A25	109.81511222
A26	109.84033204

A27	107.24151297
A28	103.53182375
A29	140.95612029
A30	109.73081908
A31	108.65675959
A32	107.87365079
A33	112.40319470
A34	109.49451378
A35	111.44035866
A36	107.14760418
A37	108.88743413
A38	111.11042214
A39	109.81771019
A40	111.90412287
D1	-0.31314026
D2	0.32751060
D3	-0.19566235
D4	178.65991442
D5	179.44273691
D6	160.35826789
D7	50.08482979
D8	65.21868424
D9	-40.86560805
D10	173.07259589
D11	171.41901636
D12	-156.27516768
D13	-76.84129286
D14	122.69448572
D15	-57.67689736
D16	179.98782657
D17	85.50367664
D18	179.66274319
D19	179.96725153
D20	-179.49480442
D21	-75.56823955
D22	-78.45731387
D23	36.88706045
D24	172.57266219
D25	-70.37021259
D26	54.40037022
D27	63.56705564
D28	-74.52685399
D29	-122.77884625
D30	121.58256797
D31	42.76741200
D32	81.89631590

D33	-36.79864884
D34	-148.19675849
D35	94.83586742
D36	-0.00955701
D37	-178.79659846
D38	61.88938727
D39	-58.65942782

1 2 1.5 6 1.5 21 1.0
2 3 1.5 22 1.0
3 4 1.5 19 1.0
4 5 1.5 23 1.0
5 6 1.5 8 1.0
6 7 1.0
7 10 1.0 12 1.0 24 1.0
8 9 1.0 25 1.0 26 1.0
9 10 1.0 27 1.0 28 1.0
10 13 1.0 29 1.0
11 12 1.0 14 1.0 30 1.0 31 1.0
12 32 1.0 33 1.0
13 14 1.0 16 1.0 34 1.0
14 15 1.0 20 1.0
15 17 1.0 18 2.0
16 17 1.0 35 1.0 36 1.0
17 37 1.0 38 1.0
18
19 39 1.0
20 40 1.0 41 1.0 42 1.0
21
22
23
24
25
26
27
28
29
30
31
32
33
34
35
36
37
38

APPENDIX B

GAUSSIAN INPUT STRUCTRUE

The following figure represents how the input file is visually translated from notepad. Each ring is labeled from left to right as A, B, C, D

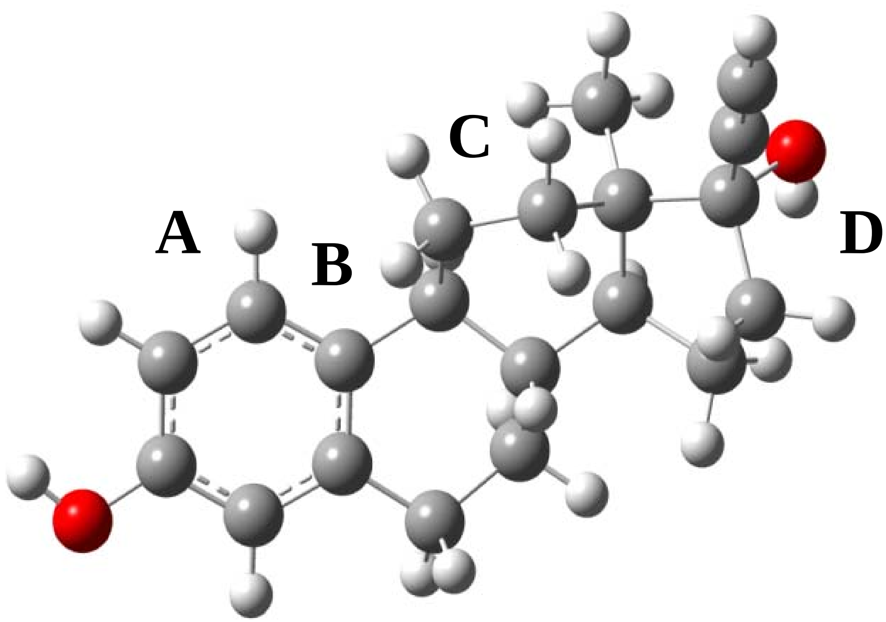

Figure 17. Gaussian Input Structure

APPENDIX C

GAUSSIAN OUTPUT FILE (OPTIMIZATION)

This section contains a small portion of the output file from Gaussian 03 after the figure given in Appendix A1 is optimized. This file contains the final iteration of the atomic charges and the calculated bond lengths. The entire optimization output file would translate to over 800 pages and as such cannot be included.

```
Atomic charges with hydrogens summed into heavy atoms:
                                                    1
    1  C   -0.051150
    2  C   -0.069898
    3  C    0.329300
    4  C   -0.066704
    5  C    0.078924
    6  C    0.078026
    7  C   -0.016447
    8  C   -0.030852
    9  C   -0.005979
   10  C    0.017388
   11  C    0.022817
   12  C    0.007055
   13  C    0.006612
   14  C   -0.022507
   15  C    0.428951
   16  C    0.000601
   17  C   -0.006180
   18  O   -0.465116
   19  O   -0.248457
   20  C    0.013615
```

21 H 0.000000
22 H 0.000000
23 H 0.000000
24 H 0.000000
25 H 0.000000
26 H 0.000000
27 H 0.000000
28 H 0.000000
29 H 0.000000
30 H 0.000000
31 H 0.000000
32 H 0.000000
33 H 0.000000
34 H 0.000000
35 H 0.000000
36 H 0.000000
37 H 0.000000
38 H 0.000000
39 H 0.000000
40 H 0.000000
41 H 0.000000
42 H 0.000000
Sum of Mulliken charges= 0.00000
Electronic spatial extent (au): <R**2>= 6697.0369
Charge= 0.0000 electrons
Dipole moment (field-independent basis, Debye):
X= -1.7158 Y= 0.6495 Z= 0.8979 Tot= 2.0425
Quadrupole moment (field-independent basis, Debye-Ang):
XX= -130.9133 YY= -113.0839 ZZ= -119.7835
XY= 18.5821 XZ= 4.3106 YZ= -1.6238
Traceless Quadrupole moment (field-independent basis, Debye-Ang):
XX= -9.6531 YY= 8.1763 ZZ= 1.4768
XY= 18.5821 XZ= 4.3106 YZ= -1.6238
Octapole moment (field-independent basis, Debye-Ang**2):
XXX= -134.4729 YYY= -6.2828 ZZZ= -4.6691 XYY= -
29.2246
XXY= -12.7060 XXZ= 24.1423 XZZ= 10.6286 YZZ=
1.7080
YYZ= 0.8925 XYZ= -7.8296
Hexadecapole moment (field-independent basis, Debye-Ang**3):
XXXX= -7125.1968 YYYY= -1398.9593 ZZZZ= -402.4347 XXXY= 669.5795
XXXZ= 113.7159 YYYX= 13.2577 YYYZ= -0.4206 ZZZX= -6.8430
ZZZY= 3.3584 XXYY= -1305.1304 XXZZ= -1252.0368 YYZZ= -310.4520

XXYZ= -24.2541 YYXZ= 8.2023 ZZXY= 0.2766
N-N= 1.578020226609D+03 E-N=-5.128653545564D+03 KE= 8.416414506965D+02
No NMR shielding tensors so no spin-rotation constants.
Leave Link 601 at Mon Sep 26 20:13:52 2011, MaxMem= 1207959552 cpu: 2.5
(Enter /usr/local/packages/g03/l9999.exe)
1\1\GINC-BL0\FOpt\RB3LYP\6-31G(d,p)\C18H22O2\WBARR\26-Sep-2011\0\\#p B
3LYP/6-31G(D,P) OPT GEOM=CONNECT\\1\\0,1\C,0.0283758632,0.1249419383,-
0.0281850015\C,-0.0182049088,-0.0292983508,1.3544933267\C,1.1714233029
,-0.2188004586,2.0630964921\C,2.3818755321,-0.2565521865,1.3727083855\
C,2.4269220835,-0.1012549166,-0.0163394728\C,1.2352771138,0.1009606969
,-0.7416580939\C,1.224048294,0.2448573754,-2.2631776906\C,3.7748316766
,-0.1385699222,-0.712419701\C,3.6585688935,-0.4363038551,-2.2086085878
\C,2.6240519894,0.4863434984,-2.8626827648\C,0.6392713864,1.9528847775
,-4.1185494075\C,0.2342541191,1.3384505471,-2.7610265671\C,2.591100650
1,0.3442554606,-4.4010611201\C,1.2949846017,0.9204910343,-5.0612527987
\C,1.7867488865,1.6303401068,-6.3404027777\C,3.7773729337,1.0641240003
,-5.1030418389\C,3.2825235246,1.391303935,-6.5163067042\O,1.0750249109
,2.2709410608,-7.0850299686\O,1.2097101743,-0.3778106062,3.4221457511\
C,0.2798268571,-0.1554117437,-5.4980850077\H,-0.9060834813,0.265666142
2,-0.5634636719\H,-0.9720964115,-0.0051082958,1.8774052853\H,3.2962596
299,-0.4129696006,1.9378895209\H,0.8827763265,-0.7211867943,-2.6678180
118\H,4.274496128,0.8320958752,-0.5776798583\H,4.419761242,-0.87727263
29,-0.2225362973\H,4.6381032187,-0.3220678034,-2.6874678384\H,3.353622
8644,-1.4815711742,-2.3583572273\H,2.9120159032,1.522179429,-2.6221854
512\H,1.3491176178,2.7717291227,-3.9466851935\H,-0.2243623708,2.404212
9167,-4.6169530831\H,-0.7740194142,0.9164796307,-2.8322098577\H,0.1768
87387,2.1402359754,-2.016572188\H,2.6472803899,-0.7271499733,-4.642330
8013\H,4.6907555768,0.4632177813,-5.0988215636\H,4.0058859996,1.996803
4856,-4.5717411111\H,3.7683514423,2.2408999596,-7.0022806371\H,3.39610
82971,0.5257259121,-7.1851194665\H,0.3085187998,-0.3350499097,3.767513
6274\H,0.7500322757,-0.9001573461,-6.1500207954\H,-0.538255574,0.31091
32554,-6.0551889422\H,-0.1430571052,-0.6885768307,-4.6423285998\\Versi
on=EM64L-G03RevE.01\State=1-A\HF=-849.6589576\RMSD=9.854e-09\RMSF=3.82
3e-06\Thermal=0.\Dipole=0.143936,-0.5171096,0.5980362\PG=C01 [X(C18H22
O2)]\\@

FAULTILY FAULTLESS, ICILY REGULAR, SPLENDIDLY NULL...
MAUDE BY TENNYSON
Job cpu time: 0 days 5 hours 20 minutes 29.0 seconds.
File lengths (MBytes): RWF= 123 Int= 0 D2E= 0 Chk= 22 Scr= 1
Normal termination of Gaussian 03 at Mon Sep 26 20:14:04 2011.

APPENDIX D

GAUSSIAN OUTPUT FILE (ENERGY)

This appendix is a portion of the output file from the energy calculation based on the optimization in appendix A3. Each of the numbers along the top represents an orbital. The column with the last O before V represents the HOMO and is the column that is used for calculating the electron density. The bottom section of the file lists all of the orbitals and is a guide to finding this set amount all of the orbitals being calculated.

```
                 71       72       73       74       75
               (A)--O   (A)--O   (A)--O   (A)--V   (A)--V
    EIGENVALUES --   -0.23972  -0.23258  -0.21128  -0.01481  -
0.00098
  1 1   C  1S      -0.00032  -0.00075  -0.00030   0.00237   0.00124
  2       2S        0.00123   0.00262   0.00145  -0.00732  -0.00376
  3       2PX       0.02424   0.00272  -0.01171  -0.00422  -0.03129
  4       2PY      -0.02205  -0.00755   0.01601   0.00454   0.03139
  5       2PZ      -0.26228  -0.01525   0.14169  -0.01774   0.32576
  6       3S       -0.00535  -0.00490  -0.01140   0.00236   0.03792
  7       3PX       0.01047   0.00163   0.00522  -0.00488   0.00229
  8       3PY      -0.02469  -0.01660   0.01311   0.03238   0.08911
  9       3PZ      -0.18680  -0.00815   0.11012  -0.02930   0.43461
 10       4XX      -0.00138   0.00025  -0.00250   0.00071  -0.00202
 11       4YY      -0.00004  -0.00031   0.00154  -0.00035   0.00015
 12       4ZZ       0.00144   0.00014   0.00065  -0.00014   0.00225
 13       4XY       0.00058   0.00022   0.00051  -0.00009   0.00205
 14       4XZ       0.00995   0.00144   0.01435  -0.00074   0.01439
 15       4YZ       0.00132   0.00023   0.00980   0.00052  -0.00198
 16 2   C  1S      -0.00008  -0.00025  -0.00008  -0.00087   0.00019
 17       2S        0.00026   0.00069  -0.00058   0.00271   0.00042
 18       2PX       0.02387   0.00324   0.01713   0.00253   0.02703
```

19	2PY	-0.02249	-0.00061	-0.01707	0.00140	-0.02381
20	2PZ	-0.27100	-0.02809	-0.20229	0.01415	-0.28203
21	3S	-0.00324	0.00330	0.01449	-0.00669	-0.00057
22	3PX	0.01480	0.00369	0.02379	-0.00254	0.05373
23	3PY	-0.01418	0.00182	-0.01305	-0.00826	-0.05945
24	3PZ	-0.20237	-0.02219	-0.16500	0.01943	-0.37692
25	4XX	0.00138	0.00005	-0.00123	-0.00017	-0.00301
26	4YY	0.00013	-0.00011	-0.00143	-0.00002	-0.00030
27	4ZZ	-0.00156	-0.00001	0.00284	-0.00010	0.00349
28	4XY	-0.00089	-0.00039	0.00195	0.00017	0.00236
29	4XZ	-0.00899	-0.00043	0.00952	-0.00105	0.01921
30	4YZ	0.00119	-0.00031	-0.01037	0.00036	-0.00284
31 3	C 1S	0.00015	0.00002	0.00000	0.00034	0.00037
32	2S	-0.00061	0.00020	0.00061	-0.00094	-0.00138
33	2PX	-0.00257	0.00066	0.02441	-0.00042	0.00520
34	2PY	0.00107	-0.00399	-0.02040	0.00274	-0.00121
35	2PZ	0.02357	-0.00694	-0.27372	0.00495	-0.04020
36	3S	-0.00200	-0.00684	-0.00702	0.00564	0.01808
37	3PX	0.00231	-0.00187	0.00647	0.00522	0.01066
38	3PY	0.00110	-0.00379	-0.01588	-0.00104	-0.02286
39	3PZ	0.01410	-0.00378	-0.16425	0.00634	-0.04540
40	4XX	-0.00061	0.00013	0.00290	0.00020	0.00054
41	4YY	0.00280	0.00012	0.00045	-0.00024	0.00387
42	4ZZ	-0.00219	-0.00026	-0.00340	0.00017	-0.00398
43	4XY	-0.00141	-0.00024	-0.00189	-0.00016	-0.00273
44	4XZ	0.00378	-0.00053	-0.01981	-0.00001	0.00212
45	4YZ	0.01998	0.00154	0.00200	-0.00152	0.02997
46 4	C 1S	-0.00070	-0.00156	0.00042	0.00043	0.00093
47	2S	0.00220	0.00318	-0.00198	-0.00071	0.00015
48	2PX	-0.02701	0.00465	0.01315	-0.00017	-0.02440
49	2PY	0.02494	0.00324	-0.01335	-0.00059	0.01885
50	2PZ	0.31608	0.01577	-0.18616	-0.01664	0.30753
51	3S	-0.00786	0.01485	0.01820	-0.00964	-0.04075
52	3PX	-0.02788	0.00133	0.01767	-0.00488	-0.05376
53	3PY	0.01938	-0.00379	-0.01967	0.00240	0.02341
54	3PZ	0.23237	0.01180	-0.14863	-0.02231	0.40447
55	4XX	-0.00162	-0.00008	-0.00128	-0.00001	0.00208
56	4YY	-0.00056	-0.00023	0.00139	0.00000	0.00086
57	4ZZ	0.00191	0.00005	0.00015	0.00012	-0.00238
58	4XY	0.00079	-0.00001	-0.00009	0.00033	-0.00138
59	4XZ	0.00977	0.00091	0.00971	0.00042	-0.01405
60	4YZ	-0.00219	0.00018	0.00954	-0.00026	0.00168
61 5	C 1S	-0.00019	-0.00048	-0.00051	-0.00073	0.00106

62		2S	-0.00145	0.00111	0.00106	0.00074	0.00452
63		2PX	-0.02697	-0.00550	-0.00962	0.00075	0.02561
64		2PY	0.02427	0.00717	0.01041	0.00361	-0.02534
65		2PZ	0.28537	0.02143	0.14121	0.01125	-0.28892
66		3S	0.01836	-0.00070	0.00225	0.01771	-0.08926
67		3PX	-0.02489	0.00557	0.01302	-0.00671	-0.05071
68		3PY	0.02313	0.01777	0.01787	-0.00973	-0.01923
69		3PZ	0.19039	0.01363	0.10650	0.01335	-0.34341
70		4XX	0.00201	0.00111	-0.00247	-0.00058	0.00311
71		4YY	-0.00110	-0.00111	-0.00092	0.00042	0.00012
72		4ZZ	-0.00120	-0.00002	0.00354	0.00016	-0.00344
73		4XY	-0.00047	0.00037	0.00215	0.00011	-0.00136
74		4XZ	-0.01255	-0.00034	0.01266	0.00118	-0.01937
75		4YZ	-0.00292	-0.00030	-0.01178	-0.00063	0.00293
76	6 C	1S	-0.00029	-0.00220	0.00140	-0.00003	0.00134
77		2S	-0.00045	0.00543	-0.00026	-0.00098	-0.00213
78		2PX	0.00296	0.01713	-0.03421	-0.00017	-0.00207
79		2PY	-0.00131	-0.00389	0.02555	0.00256	-0.00444
80		2PZ	0.02147	0.01018	0.31545	0.00931	-0.04374
81		3S	0.01694	0.01390	-0.03571	-0.00875	-0.01679
82		3PX	-0.00374	-0.01248	-0.04519	0.03622	0.02372
83		3PY	-0.01042	-0.00203	0.02061	0.00748	0.10413
84		3PZ	0.02443	0.00774	0.22388	0.01437	-0.07607
85		4XX	0.00020	0.00041	0.00088	0.00003	0.00035
86		4YY	0.00266	0.00017	0.00028	-0.00042	-0.00413
87		4ZZ	-0.00243	-0.00034	-0.00145	0.00004	0.00353
88		4XY	-0.00123	-0.00014	-0.00036	-0.00042	0.00185
89		4XZ	-0.00015	-0.00001	-0.00800	0.00037	-0.00321
90		4YZ	0.01714	0.00102	0.00089	0.00165	-0.02974
91	7 C	1S	-0.00103	-0.00363	-0.00127	0.00585	0.00359
92		2S	0.00163	0.00648	0.00506	-0.00753	-0.00088
93		2PX	-0.00038	-0.00465	0.01519	-0.01050	-0.00360
94		2PY	0.00875	-0.00221	0.00325	0.01046	-0.00890
95		2PZ	-0.00534	-0.01465	-0.08480	0.00740	-0.01364
96		3S	0.01188	0.02901	0.02093	-0.09376	-0.10149
97		3PX	0.00858	-0.01070	-0.03215	-0.00097	-0.03972
98		3PY	0.03428	-0.00248	0.00280	-0.00690	-0.17233
99		3PZ	-0.00549	-0.01443	-0.02184	0.01401	-0.02862
100		4XX	0.00050	0.00235	0.00315	-0.00029	-0.00096
101		4YY	0.00037	-0.00148	0.00523	0.00028	-0.00231
102		4ZZ	-0.00103	-0.00097	-0.00782	0.00040	0.00308
103		4XY	0.00011	-0.00026	-0.00099	0.00111	0.00042
104		4XZ	-0.00074	-0.00160	-0.01302	-0.00040	0.00217

105	4YZ	0.00062	0.00043	0.00396	-0.00025	-0.00368
106 8	C 1S	0.00153	-0.00328	0.00096	0.00043	-0.00253
107	2S	-0.00449	0.00808	0.00052	0.00023	-0.00251
108	2PX	0.00983	0.02807	-0.00730	-0.00429	0.01029
109	2PY	-0.01099	-0.00892	0.00006	0.00112	-0.00931
110	2PZ	-0.10059	-0.00191	-0.03232	-0.00255	-0.01473
111	3S	-0.01193	0.00543	-0.03055	-0.01090	0.10076
112	3PX	0.01960	0.02015	-0.02183	-0.02015	0.07260
113	3PY	-0.00376	0.00331	0.02480	0.00392	-0.09849
114	3PZ	-0.03191	0.00147	-0.01195	-0.00286	-0.08047
115	4XX	-0.00295	-0.00025	-0.00144	-0.00047	0.00281
116	4YY	-0.00374	-0.00122	-0.00124	-0.00003	0.00367
117	4ZZ	0.00658	0.00062	0.00268	0.00029	-0.00623
118	4XY	0.00336	0.00178	0.00138	0.00076	-0.00338
119	4XZ	-0.00548	0.00061	-0.00181	0.00002	0.00581
120	4YZ	-0.01253	-0.00125	-0.00633	-0.00070	0.01657
121 9	C 1S	0.00623	0.00395	0.00040	-0.00319	-0.00792
122	2S	-0.01551	-0.00835	-0.00923	0.00229	0.03195
123	2PX	0.03070	-0.02442	0.02424	0.00622	-0.01951
124	2PY	0.00425	0.03037	-0.00208	0.00960	0.00749
125	2PZ	0.03095	0.00425	-0.00060	0.00300	0.00301
126	3S	-0.02910	-0.01409	0.04816	0.05425	-0.02118
127	3PX	0.02924	-0.01284	0.00299	-0.00762	0.03937
128	3PY	-0.02608	0.01835	-0.03710	0.01800	0.12814
129	3PZ	-0.00579	0.00366	-0.01672	-0.01396	0.06811
130	4XX	-0.00329	0.00216	-0.00134	-0.00031	-0.00081
131	4YY	0.00024	-0.00111	0.00148	-0.00003	-0.00087
132	4ZZ	0.00386	-0.00040	-0.00116	-0.00083	0.00208
133	4XY	0.00207	-0.00030	0.00130	-0.00010	-0.00195
134	4XZ	0.00090	0.00135	0.00025	-0.00049	0.00138
135	4YZ	-0.00128	-0.00123	-0.00030	0.00000	0.00206
136 10	C 1S	0.00394	-0.00580	-0.00513	-0.00701	-0.00310
137	2S	-0.00206	0.01087	0.01284	0.00821	-0.01412
138	2PX	-0.00021	0.06253	-0.02164	0.01211	-0.00503
139	2PY	-0.01731	-0.01675	-0.03105	-0.00576	0.00027
140	2PZ	-0.01069	0.01016	0.01161	0.00195	0.00370
141	3S	-0.06439	0.02691	0.02589	0.08805	0.18939
142	3PX	0.02312	0.04130	0.02855	0.02296	-0.14611
143	3PY	-0.01248	-0.00870	-0.04898	-0.04559	-0.03594
144	3PZ	-0.00919	0.00591	-0.01738	0.02831	0.03006
145	4XX	-0.00064	0.00139	-0.00076	-0.00141	0.00162
146	4YY	-0.00009	-0.00200	0.00288	-0.00030	0.00050
147	4ZZ	0.00188	-0.00030	-0.00230	-0.00146	-0.00334

148			4XY	0.00091	0.00266	0.00109	-0.00054	-0.00060
149			4XZ	-0.00025	0.00211	0.00012	0.00040	0.00167
150			4YZ	-0.00005	0.00034	0.00197	0.00032	0.00103
151	11	C	1S	-0.00089	0.00068	0.00523	-0.03162	0.00127
152			2S	-0.00040	-0.00458	-0.00955	0.05058	0.00385
153			2PX	-0.00436	-0.04631	0.04121	0.05241	0.01029
154			2PY	0.00155	-0.04546	-0.00337	0.08294	0.00703
155			2PZ	-0.00155	-0.01081	-0.01256	0.05147	-0.00381
156			3S	0.02227	0.03263	-0.04662	0.34395	-0.06767
157			3PX	-0.01102	-0.03882	0.03670	0.03667	0.04455
158			3PY	0.00138	-0.05081	0.00670	0.14062	0.01621
159			3PZ	0.00388	-0.00440	-0.01193	0.05352	-0.02378
160			4XX	-0.00039	0.00695	-0.00051	-0.00672	-0.00084
161			4YY	-0.00006	-0.00143	0.00090	-0.00095	0.00059
162			4ZZ	0.00036	-0.00633	0.00021	0.00223	0.00013
163			4XY	-0.00030	0.00291	-0.00289	-0.00343	0.00055
164			4XZ	-0.00069	0.00005	-0.00040	0.00306	0.00187
165			4YZ	-0.00028	-0.00173	0.00056	0.00187	0.00054
166	12	C	1S	0.00247	-0.00773	-0.01373	0.01174	0.00035
167			2S	-0.00497	0.02063	0.02668	-0.02144	0.00176
168			2PX	0.00769	0.06620	-0.05735	-0.04731	-0.01152
169			2PY	-0.00141	0.02414	0.04554	-0.00400	-0.01349
170			2PZ	0.01478	-0.00332	0.02481	0.00575	-0.03224
171			3S	-0.01273	0.00927	0.09795	-0.11422	-0.02351
172			3PX	-0.01719	0.03223	-0.01438	-0.06793	0.08080
173			3PY	-0.00410	0.01014	0.03325	0.01755	0.00520
174			3PZ	0.02595	-0.00578	-0.00222	0.01219	-0.10785
175			4XX	0.00023	0.00057	-0.00338	0.00198	-0.00103
176			4YY	0.00083	-0.00032	0.00321	0.00040	0.00012
177			4ZZ	-0.00084	-0.00162	-0.00149	-0.00008	0.00165
178			4XY	-0.00009	-0.00190	-0.00041	0.00354	0.00031
179			4XZ	-0.00050	-0.00290	0.00018	0.00289	0.00051
180			4YZ	-0.00060	-0.00009	0.00097	-0.00125	-0.00021
181	13	C	1S	0.00131	0.00081	-0.00002	-0.00646	-0.00540
182			2S	-0.00216	0.00513	0.00272	-0.00108	0.00550
183			2PX	0.00918	-0.05189	0.01152	0.01673	-0.01395
184			2PY	-0.00424	0.06822	-0.00506	0.00847	0.00092
185			2PZ	-0.00227	0.01202	0.00553	0.00661	-0.00504
186			3S	-0.00719	-0.06187	-0.02193	0.16898	0.09027
187			3PX	0.00753	-0.04576	0.01890	0.11728	-0.02442
188			3PY	-0.00564	0.06517	0.01142	0.05959	0.00425
189			3PZ	0.00052	0.00907	0.01916	-0.04628	-0.03387
190			4XX	-0.00035	0.00595	-0.00001	0.00467	-0.00031

191		4YY	0.00084	-0.00850	0.00031	-0.00125	-0.00038
192		4ZZ	0.00016	0.00302	0.00004	-0.00440	-0.00106
193		4XY	0.00044	-0.00256	0.00035	0.00398	0.00029
194		4XZ	0.00000	0.00001	-0.00049	0.00145	-0.00020
195		4YZ	-0.00007	0.00207	0.00035	0.00070	-0.00016
196	14 C	1S	0.00299	-0.02262	0.00040	0.00078	-0.00219
197		2S	-0.00424	0.03694	-0.00353	0.00064	0.00294
198		2PX	-0.01373	0.25231	-0.00661	0.00234	-0.00308
199		2PY	0.00112	0.01891	0.00034	-0.00779	-0.00890
200		2PZ	0.01198	-0.08910	0.00677	-0.01196	-0.00935
201		3S	-0.02635	0.20926	0.01252	-0.02051	0.01988
202		3PX	-0.00685	0.17974	-0.01056	0.06465	-0.01084
203		3PY	-0.00063	0.06610	0.00202	-0.03941	-0.02949
204		3PZ	0.00709	-0.05589	0.00483	0.21385	0.00830
205		4XX	-0.00021	0.00697	-0.00176	0.01436	0.00023
206		4YY	0.00056	-0.00652	0.00084	-0.00080	-0.00051
207		4ZZ	0.00023	-0.00319	0.00041	-0.01329	-0.00034
208		4XY	-0.00017	0.00352	-0.00077	0.00381	-0.00066
209		4XZ	0.00027	-0.00473	-0.00021	0.01998	0.00121
210		4YZ	-0.00021	-0.00183	0.00038	0.01314	0.00064
211	15 C	1S	0.00004	-0.00561	0.00157	0.00168	0.00078
212		2S	-0.00072	0.01530	-0.00349	0.00280	-0.00049
213		2PX	0.00769	-0.13293	0.00987	0.17187	0.01213
214		2PY	0.00729	-0.12024	0.00409	-0.02949	0.00020
215		2PZ	-0.00200	0.04230	-0.00112	0.46218	0.02173
216		3S	0.00053	0.02037	-0.00795	-0.08406	-0.00545
217		3PX	-0.00405	0.02404	0.00435	0.12965	0.00817
218		3PY	-0.00312	0.01226	-0.00199	-0.06198	0.00636
219		3PZ	0.00046	-0.01274	0.00081	0.41979	0.02532
220		4XX	-0.00266	0.03311	-0.00064	-0.01037	-0.00003
221		4YY	0.00261	-0.03739	0.00109	-0.00274	0.00038
222		4ZZ	-0.00023	0.00424	-0.00025	0.01204	0.00058
223		4XY	-0.00011	0.00012	0.00001	0.00897	0.00147
224		4XZ	0.00075	-0.01419	0.00067	-0.01570	-0.00029
225		4YZ	0.00028	-0.00278	0.00013	0.01980	0.00071
226	16 C	1S	0.00022	0.00034	-0.00050	-0.01468	-0.00539
227		2S	0.00019	-0.00732	0.00175	0.05188	0.00868
228		2PX	-0.00665	0.06598	-0.00493	0.04539	0.00037
229		2PY	-0.00007	-0.02866	-0.00206	-0.00156	0.00452
230		2PZ	0.00471	-0.03481	-0.00304	-0.00734	-0.00603
231		3S	-0.00341	0.04786	-0.00131	0.02301	0.04889
232		3PX	-0.00459	0.07334	-0.00218	0.06464	0.00776
233		3PY	-0.00053	-0.03400	-0.00292	0.20242	0.02291

234			3PZ	0.00394	-0.01701	-0.00521	-0.06165	-0.01776
235			4XX	-0.00036	0.00613	-0.00060	0.00190	-0.00092
236			4YY	0.00069	-0.00780	0.00045	-0.00562	-0.00084
237			4ZZ	0.00000	0.00013	0.00050	0.00405	-0.00024
238			4XY	-0.00030	0.00386	-0.00008	0.00031	0.00046
239			4XZ	-0.00011	0.00066	0.00005	0.00017	-0.00024
240			4YZ	0.00011	-0.00219	-0.00025	-0.00659	-0.00017
241	17	C	1S	-0.00189	0.02956	-0.00037	-0.00358	-0.00053
242			2S	0.00369	-0.05431	0.00058	-0.00327	0.00095
243			2PX	0.00145	-0.00404	0.00305	-0.01042	0.00387
244			2PY	-0.01666	0.24346	-0.00902	-0.00347	-0.00496
245			2PZ	-0.00285	0.02607	0.00000	-0.00363	0.00050
246			3S	0.01445	-0.23424	0.00490	0.11718	0.00263
247			3PX	-0.00010	0.03082	0.00144	-0.04905	0.00903
248			3PY	-0.01211	0.16445	-0.00784	-0.08616	-0.00845
249			3PZ	-0.00219	0.02753	-0.00075	0.17046	0.00717
250			4XX	-0.00037	0.00561	-0.00007	0.00136	0.00018
251			4YY	0.00030	-0.00487	0.00004	0.00359	0.00024
252			4ZZ	-0.00018	0.00411	0.00001	-0.00548	-0.00060
253			4XY	0.00019	0.00000	-0.00004	-0.01017	-0.00108
254			4XZ	-0.00023	0.00053	0.00002	-0.01422	-0.00012
255			4YZ	-0.00003	-0.00054	-0.00006	-0.02736	-0.00127
256	18	O	1S	0.00002	-0.00044	0.00025	-0.00117	0.00020
257			2S	-0.00013	0.00485	-0.00072	-0.00061	-0.00213
258			2PX	-0.02747	0.35134	-0.00739	-0.14158	-0.00647
259			2PY	-0.02738	0.36620	-0.00790	0.02164	-0.00116
260			2PZ	0.00549	-0.10782	0.00821	-0.36222	-0.01900
261			3S	0.00021	-0.01435	-0.00134	0.02304	0.00622
262			3PX	-0.01958	0.25965	-0.00607	-0.14184	-0.00880
263			3PY	-0.01955	0.26444	-0.00659	0.03560	0.00025
264			3PZ	0.00390	-0.07863	0.00544	-0.36580	-0.01862
265			4XX	0.00091	-0.01071	0.00015	-0.00205	-0.00037
266			4YY	-0.00103	0.01390	-0.00024	-0.00030	-0.00039
267			4ZZ	0.00004	-0.00017	0.00001	-0.00046	-0.00045
268			4XY	-0.00002	-0.00013	0.00018	0.00051	0.00014
269			4XZ	-0.00036	0.00517	-0.00013	-0.00182	-0.00008
270			4YZ	-0.00016	0.00115	0.00024	0.00242	0.00010
271	19	O	1S	-0.00010	-0.00029	0.00034	-0.00008	-0.00040
272			2S	-0.00015	0.00049	-0.00030	0.00011	0.00148
273			2PX	0.00299	-0.00091	-0.02678	0.00128	0.00070
274			2PY	-0.00242	0.00172	0.02354	-0.00108	0.00048
275			2PZ	-0.03488	0.00924	0.29547	-0.00235	0.01914
276			3S	0.00265	0.00205	-0.00481	0.00196	0.00226

277	3PX	0.00309	-0.00066	-0.02226	0.00172	-0.00002
278	3PY	-0.00251	0.00136	0.02020	-0.00062	0.00219
279	3PZ	-0.02894	0.00731	0.24145	-0.00245	0.01948
280	4XX	-0.00011	-0.00005	0.00051	-0.00007	0.00002
281	4YY	0.00034	-0.00020	-0.00120	-0.00001	0.00076
282	4ZZ	-0.00054	-0.00002	0.00117	0.00001	-0.00053
283	4XY	-0.00033	-0.00007	0.00082	0.00014	-0.00036
284	4XZ	0.00017	0.00000	-0.00226	0.00010	-0.00056
285	4YZ	0.00333	-0.00015	-0.00977	-0.00018	0.00471
286 20	C 1S	-0.00049	0.00238	-0.00255	0.02916	0.00255
287	2S	0.00115	-0.00669	0.00542	-0.04882	-0.00306
288	2PX	0.00038	-0.02721	-0.01685	0.00719	0.00709
289	2PY	0.00351	-0.04081	0.00162	-0.07177	-0.00005
290	2PZ	-0.00443	0.03273	0.00122	0.07093	0.00028
291	3S	0.00295	0.00689	0.01372	-0.31719	-0.04227
292	3PX	-0.00084	-0.01123	-0.01156	0.05890	0.01931
293	3PY	0.00393	-0.05442	-0.00566	-0.14315	-0.00046
294	3PZ	-0.00390	0.02610	0.00437	0.09042	0.00506
295	4XX	-0.00006	0.00156	-0.00022	0.00639	0.00048
296	4YY	0.00019	-0.00158	-0.00023	0.00048	-0.00028
297	4ZZ	-0.00006	0.00018	-0.00015	-0.00071	0.00018
298	4XY	-0.00030	0.00533	0.00044	0.00609	0.00016
299	4XZ	0.00044	-0.00755	-0.00050	-0.00563	-0.00037
300	4YZ	-0.00004	-0.00160	-0.00026	-0.00118	0.00019
301 21	H 1S	0.00006	0.00210	-0.00101	-0.00283	-0.00098
302	2S	-0.00534	-0.01060	0.00273	0.02997	0.02884
303	3PX	0.00083	-0.00027	-0.00046	0.00071	-0.00167
304	3PY	-0.00064	-0.00001	0.00037	-0.00009	0.00099
305	3PZ	-0.00703	-0.00027	0.00366	-0.00084	0.01238
306 22	H 1S	-0.00017	-0.00194	0.00100	0.00045	0.00089
307	2S	0.00009	-0.00202	0.00280	-0.00238	-0.00139
308	3PX	0.00070	0.00009	0.00031	0.00001	0.00065
309	3PY	-0.00063	-0.00009	-0.00040	0.00003	-0.00088
310	3PZ	-0.00736	-0.00074	-0.00535	0.00050	-0.01087
311 23	H 1S	0.00051	0.00004	0.00064	-0.00020	0.00086
312	2S	-0.00236	-0.00162	0.00446	-0.00320	0.01073
313	3PX	-0.00066	0.00002	0.00035	0.00011	-0.00070
314	3PY	0.00043	-0.00003	-0.00039	-0.00004	0.00132
315	3PZ	0.00782	0.00038	-0.00468	-0.00063	0.01179
316 24	H 1S	-0.00631	-0.00798	-0.08202	0.00051	0.01276
317	2S	-0.01265	-0.00663	-0.10921	0.00828	0.08528
318	3PX	0.00003	-0.00031	-0.00136	-0.00086	0.00009
319	3PY	0.00016	-0.00005	-0.00034	-0.00044	-0.00027

320			3PZ	0.00012	0.00008	0.00119	0.00055	0.00017
321	25	H	1S	0.08925	0.00677	0.03363	0.00297	-0.05782
322			2S	0.11467	0.00563	0.05102	0.00521	-0.22062
323			3PX	0.00117	0.00056	0.00004	-0.00010	-0.00142
324			3PY	0.00030	-0.00019	0.00029	0.00016	-0.00237
325			3PZ	0.00152	0.00017	0.00057	0.00005	-0.00050
326	26	H	1S	-0.05808	-0.01704	-0.01959	-0.00360	0.04087
327			2S	-0.06141	-0.02476	-0.04508	-0.01565	0.19610
328			3PX	-0.00219	0.00028	-0.00037	0.00012	0.00036
329			3PY	0.00004	0.00010	0.00029	0.00005	0.00073
330			3PZ	-0.00114	0.00037	-0.00052	-0.00004	-0.00002
331	27	H	1S	0.00608	0.00036	0.01088	0.00314	-0.01363
332			2S	0.02039	-0.00806	0.02870	-0.02739	-0.11500
333			3PX	0.00011	-0.00084	0.00018	-0.00070	-0.00062
334			3PY	0.00013	0.00047	-0.00024	-0.00014	0.00027
335			3PZ	0.00088	0.00019	0.00034	0.00023	0.00022
336	28	H	1S	0.02272	-0.00256	-0.00457	-0.00019	0.00954
337			2S	0.05309	0.00019	0.00126	-0.00874	-0.04362
338			3PX	0.00048	-0.00020	0.00022	-0.00016	0.00063
339			3PY	0.00018	0.00044	0.00015	0.00017	0.00066
340			3PZ	-0.00034	0.00022	0.00002	-0.00029	-0.00012
341	29	H	1S	0.00800	-0.00411	-0.01291	-0.00143	-0.01413
342			2S	0.01686	-0.00720	-0.04511	-0.00771	-0.02902
343			3PX	-0.00022	0.00098	-0.00053	-0.00020	-0.00043
344			3PY	0.00002	-0.00038	-0.00008	-0.00001	-0.00085
345			3PZ	-0.00006	0.00006	-0.00030	0.00078	0.00008
346	30	H	1S	0.00386	-0.02048	0.00087	0.01287	-0.00211
347			2S	0.00470	-0.02616	-0.00082	-0.11168	-0.02365
348			3PX	0.00001	-0.00045	0.00071	-0.00284	-0.00047
349			3PY	0.00003	0.00009	-0.00026	-0.00099	-0.00030
350			3PZ	0.00002	-0.00028	-0.00020	0.00052	-0.00002
351	31	H	1S	-0.00057	-0.00077	0.01773	-0.00408	-0.00203
352			2S	0.00392	-0.05625	0.02889	0.01291	-0.00327
353			3PX	0.00015	-0.00228	0.00063	0.00165	-0.00026
354			3PY	0.00008	-0.00147	0.00059	0.00162	-0.00012
355			3PZ	-0.00007	-0.00035	-0.00008	0.00153	0.00013
356	32	H	1S	0.00419	-0.01053	0.00263	0.00880	0.00635
357			2S	-0.00040	-0.00972	0.00277	0.05929	0.06325
358			3PX	0.00050	0.00168	-0.00148	-0.00129	-0.00133
359			3PY	-0.00027	0.00012	0.00083	0.00013	0.00094
360			3PZ	0.00000	0.00044	0.00038	0.00044	0.00016
361	33	H	1S	-0.01136	-0.02315	0.00322	0.01417	0.01091
362			2S	0.00679	-0.03554	-0.04120	0.04872	-0.05797

363		3PX	-0.00053	0.00111	0.00027	-0.00166	0.00155
364		3PY	-0.00003	0.00051	0.00007	-0.00043	-0.00022
365		3PZ	0.00000	-0.00084	0.00069	0.00084	-0.00037
366	34 H	1S	-0.00184	0.02352	0.00221	-0.01111	-0.00140
367		2S	0.00057	0.03145	-0.00889	-0.06136	-0.00388
368		3PX	0.00003	-0.00100	0.00038	0.00007	-0.00057
369		3PY	0.00015	0.00105	0.00000	-0.00057	-0.00028
370		3PZ	0.00019	-0.00087	0.00000	-0.00031	-0.00034
371	35 H	1S	0.00316	-0.04851	-0.00050	-0.02875	0.00023
372		2S	0.00523	-0.05955	0.00192	-0.21415	-0.03170
373		3PX	-0.00031	0.00180	-0.00023	0.00041	0.00052
374		3PY	-0.00003	0.00083	0.00006	-0.00040	-0.00027
375		3PZ	0.00007	-0.00005	0.00000	0.00020	-0.00015
376	36 H	1S	-0.00144	0.00955	0.00361	0.01891	0.00148
377		2S	0.00078	0.01594	0.00402	-0.03507	-0.03892
378		3PX	-0.00021	0.00106	0.00011	0.00057	0.00064
379		3PY	0.00000	-0.00038	0.00006	0.00085	0.00010
380		3PZ	0.00004	-0.00027	0.00018	0.00003	0.00001
381	37 H	1S	0.00068	0.01229	-0.00031	0.06561	0.00063
382		2S	-0.00242	0.06293	-0.00186	0.25505	0.00067
383		3PX	0.00002	-0.00051	0.00009	-0.00128	0.00001
384		3PY	-0.00024	0.00375	-0.00014	0.00231	-0.00002
385		3PZ	-0.00006	0.00080	-0.00003	0.00006	0.00011
386	38 H	1S	-0.00255	0.03073	-0.00004	-0.10934	-0.00424
387		2S	-0.00445	0.05383	-0.00001	-0.34741	-0.01885
388		3PX	0.00006	-0.00087	0.00005	0.00045	0.00025
389		3PY	-0.00033	0.00513	-0.00024	-0.00547	-0.00047
390		3PZ	0.00006	-0.00065	0.00001	0.00094	-0.00008
391	39 H	1S	-0.00030	-0.00075	0.00070	0.00050	-0.00022
392		2S	-0.00018	-0.00152	0.00147	0.00053	-0.00130
393		3PX	0.00015	-0.00004	-0.00089	0.00001	0.00018
394		3PY	-0.00016	0.00005	0.00083	0.00000	-0.00004
395		3PZ	-0.00179	0.00026	0.00987	0.00000	-0.00105
396	40 H	1S	0.00000	-0.01770	-0.00243	-0.01242	0.00068
397		2S	-0.00036	-0.02154	-0.00352	0.05601	0.00324
398		3PX	0.00005	-0.00056	-0.00039	0.00193	0.00019
399		3PY	0.00007	0.00001	0.00020	0.00029	-0.00013
400		3PZ	-0.00006	0.00073	-0.00003	-0.00063	-0.00002
401	41 H	1S	0.00039	-0.01081	-0.00475	-0.00732	-0.00075
402		2S	0.00421	-0.07157	-0.00606	-0.06350	-0.00153
403		3PX	0.00009	-0.00158	-0.00019	0.00007	0.00015
404		3PY	0.00011	-0.00173	-0.00013	-0.00187	0.00004
405		3PZ	-0.00017	0.00178	-0.00025	0.00186	-0.00003

406 42	H 1S	-0.00278	0.04754	0.00709	0.03887	0.00181
407	2S	-0.00425	0.06513	-0.01065	0.15254	0.03055
408	3PX	-0.00003	0.00090	0.00075	-0.00001	-0.00046
409	3PY	0.00000	-0.00060	-0.00024	-0.00213	0.00012
410	3PZ	-0.00013	0.00070	0.00005	0.00214	0.00017

1	(A)--O	-19.17528	29.02622
2	(A)--O	-19.13522	29.02542
3	(A)--O	-10.26542	15.88665
4	(A)--O	-10.24389	15.88486
5	(A)--O	-10.19718	15.89180
6	(A)--O	-10.19239	15.88150
7	(A)--O	-10.19118	15.88880
8	(A)--O	-10.19117	15.89001
9	(A)--O	-10.19089	15.88344
10	(A)--O	-10.19047	15.88811
11	(A)--O	-10.18821	15.88979
12	(A)--O	-10.18645	15.88593
13	(A)--O	-10.18620	15.87674
14	(A)--O	-10.18502	15.88213
15	(A)--O	-10.18452	15.88431
16	(A)--O	-10.18406	15.88674
17	(A)--O	-10.18350	15.88639
18	(A)--O	-10.18282	15.88696
19	(A)--O	-10.17975	15.88381
20	(A)--O	-10.17692	15.87986
21	(A)--O	-1.05516	2.55112
22	(A)--O	-1.03438	2.65831
23	(A)--O	-0.86850	1.34878
24	(A)--O	-0.84864	1.45118
25	(A)--O	-0.80714	1.45256
26	(A)--O	-0.79205	1.35629
27	(A)--O	-0.76452	1.46857
28	(A)--O	-0.74300	1.56793
29	(A)--O	-0.72868	1.57599
30	(A)--O	-0.71115	1.49350
31	(A)--O	-0.68258	1.51817
32	(A)--O	-0.65446	1.46871
33	(A)--O	-0.63078	1.43434
34	(A)--O	-0.61485	1.43495
35	(A)--O	-0.60767	1.52326
36	(A)--O	-0.58241	1.35964

37	(A)--O	-0.56898	1.58912
38	(A)--O	-0.55137	1.22770
39	(A)--O	-0.52208	1.37705
40	(A)--O	-0.50200	1.36134
41	(A)--O	-0.48635	1.10525
42	(A)--O	-0.47970	1.32353
43	(A)--O	-0.47873	1.35044
44	(A)--O	-0.45790	1.13578
45	(A)--O	-0.45257	1.38049
46	(A)--O	-0.44619	1.37391
47	(A)--O	-0.43423	1.38351
48	(A)--O	-0.43211	1.10714
49	(A)--O	-0.42355	1.25733
50	(A)--O	-0.41403	1.15974
51	(A)--O	-0.40599	1.29947
52	(A)--O	-0.40257	1.26429
53	(A)--O	-0.39928	1.46413
54	(A)--O	-0.39574	1.34412
55	(A)--O	-0.38949	1.34044
56	(A)--O	-0.38167	1.55830
57	(A)--O	-0.37874	1.49653
58	(A)--O	-0.37175	1.29307
59	(A)--O	-0.36249	1.36612
60	(A)--O	-0.35850	1.45025
61	(A)--O	-0.34898	1.53749
62	(A)--O	-0.34366	1.34653
63	(A)--O	-0.34212	1.45914
64	(A)--O	-0.33764	1.26371
65	(A)--O	-0.33129	1.44632
66	(A)--O	-0.32298	1.46356
67	(A)--O	-0.31469	1.41012
68	(A)--O	-0.30291	1.45306
69	(A)--O	-0.29751	1.47310
70	(A)--O	-0.28710	1.47220
71	(A)--O	-0.23972	1.16113
72	(A)--O	-0.23258	2.16130
73	(A)--O	-0.21128	1.51128
74	(A)--V	-0.01481	1.83246
75	(A)--V	-0.00098	1.32035
76	(A)--V	0.01682	1.54228
77	(A)--V	0.07185	1.24385
78	(A)--V	0.07658	0.94978
79	(A)--V	0.08285	0.88177

80	(A)--V	0.09968	0.99628
81	(A)--V	0.10139	1.03677
82	(A)--V	0.10683	1.15611
83	(A)--V	0.12649	1.08419
84	(A)--V	0.13267	1.08791
85	(A)--V	0.13776	0.98481
86	(A)--V	0.14574	1.02335
87	(A)--V	0.14725	1.21310
88	(A)--V	0.14955	1.13714
89	(A)--V	0.15751	1.20783
90	(A)--V	0.16299	1.25424
91	(A)--V	0.16387	1.26663
92	(A)--V	0.17295	1.44188
93	(A)--V	0.17621	1.23505
94	(A)--V	0.18887	1.30912
95	(A)--V	0.19153	1.39881
96	(A)--V	0.19192	1.28593
97	(A)--V	0.19561	1.21074
98	(A)--V	0.20252	1.62794
99	(A)--V	0.20823	1.29511
100	(A)--V	0.21574	1.52954
101	(A)--V	0.22502	1.53841
102	(A)--V	0.22625	1.32706
103	(A)--V	0.23999	1.32237
104	(A)--V	0.24545	1.91401
105	(A)--V	0.24627	1.69960
106	(A)--V	0.25211	1.54374
107	(A)--V	0.25495	1.66393
108	(A)--V	0.26284	1.81692
109	(A)--V	0.27054	1.87850
110	(A)--V	0.28546	1.78573
111	(A)--V	0.29759	1.79833
112	(A)--V	0.30082	1.72403
113	(A)--V	0.32042	1.89782
114	(A)--V	0.34040	1.89969
115	(A)--V	0.34477	1.82538
116	(A)--V	0.35599	1.73691
117	(A)--V	0.36372	2.01359
118	(A)--V	0.37035	2.02464
119	(A)--V	0.38993	2.18610
120	(A)--V	0.40346	2.07995
121	(A)--V	0.48152	1.78896
122	(A)--V	0.49274	2.04923

123	(A)--V	0.50987	2.00693
124	(A)--V	0.51364	1.88167
125	(A)--V	0.51728	1.99296
126	(A)--V	0.52248	1.99542
127	(A)--V	0.53219	2.16485
128	(A)--V	0.54273	1.93830
129	(A)--V	0.54861	1.96599
130	(A)--V	0.55775	2.01199
131	(A)--V	0.55886	2.14422
132	(A)--V	0.57351	2.19723
133	(A)--V	0.57523	2.05275
134	(A)--V	0.58851	2.22883
135	(A)--V	0.59480	2.32924
136	(A)--V	0.59833	2.24796
137	(A)--V	0.60921	2.19048
138	(A)--V	0.61040	2.45112
139	(A)--V	0.61679	2.45123
140	(A)--V	0.62713	2.37933
141	(A)--V	0.63012	2.23986
142	(A)--V	0.63398	2.52449
143	(A)--V	0.63832	2.32017
144	(A)--V	0.65600	2.32249
145	(A)--V	0.66067	2.34389
146	(A)--V	0.66386	2.43729
147	(A)--V	0.67945	2.54688
148	(A)--V	0.68386	2.80088
149	(A)--V	0.69839	2.54753
150	(A)--V	0.70216	2.43342
151	(A)--V	0.71304	2.57812
152	(A)--V	0.72647	2.39331
153	(A)--V	0.72981	2.38796
154	(A)--V	0.73965	2.28644
155	(A)--V	0.74484	2.66693
156	(A)--V	0.75324	2.37392
157	(A)--V	0.75820	2.34024
158	(A)--V	0.76789	2.41420
159	(A)--V	0.78612	2.39867
160	(A)--V	0.79781	2.30466
161	(A)--V	0.79968	2.44269
162	(A)--V	0.80356	2.50322
163	(A)--V	0.81041	2.63820
164	(A)--V	0.81993	2.51969
165	(A)--V	0.82252	2.48095

166	(A)--V	0.83130	2.39665
167	(A)--V	0.84025	2.46069
168	(A)--V	0.84327	2.43528
169	(A)--V	0.84635	2.55040
170	(A)--V	0.85215	2.46400
171	(A)--V	0.85840	2.42595
172	(A)--V	0.86752	2.52093
173	(A)--V	0.87017	2.60678
174	(A)--V	0.88181	2.37951
175	(A)--V	0.88576	2.31625
176	(A)--V	0.89191	2.46086
177	(A)--V	0.90402	2.42356
178	(A)--V	0.90667	2.42584
179	(A)--V	0.91282	2.43727
180	(A)--V	0.91484	2.36395
181	(A)--V	0.92144	2.46551
182	(A)--V	0.92827	2.46962
183	(A)--V	0.93074	2.44607
184	(A)--V	0.94278	2.47057
185	(A)--V	0.95281	2.89090
186	(A)--V	0.96415	2.67408
187	(A)--V	0.97451	2.53776
188	(A)--V	0.97596	2.57479
189	(A)--V	0.97935	2.51502
190	(A)--V	0.99629	2.34999
191	(A)--V	1.00345	2.50081
192	(A)--V	1.00635	2.57668
193	(A)--V	1.02224	2.67674
194	(A)--V	1.04632	2.50025
195	(A)--V	1.06526	2.72629
196	(A)--V	1.07079	2.51143
197	(A)--V	1.10367	2.54806
198	(A)--V	1.10839	2.50996
199	(A)--V	1.11839	2.84062
200	(A)--V	1.12627	2.49244
201	(A)--V	1.14858	2.46369
202	(A)--V	1.15734	2.34993
203	(A)--V	1.18101	2.39806
204	(A)--V	1.19130	2.40304
205	(A)--V	1.20319	2.44813
206	(A)--V	1.21585	2.59073
207	(A)--V	1.24401	2.42436
208	(A)--V	1.24817	2.40136

209	(A)--V	1.27798	2.43269
210	(A)--V	1.28774	2.59958
211	(A)--V	1.30440	2.57877
212	(A)--V	1.31407	2.49559
213	(A)--V	1.34029	2.47450
214	(A)--V	1.34434	2.46873
215	(A)--V	1.38966	2.51212
216	(A)--V	1.39572	2.55839
217	(A)--V	1.40862	2.53985
218	(A)--V	1.41177	2.54481
219	(A)--V	1.43273	2.55207
220	(A)--V	1.44227	2.59055
221	(A)--V	1.46392	2.57322
222	(A)--V	1.47317	2.64340
223	(A)--V	1.51251	2.62851
224	(A)--V	1.52023	2.73058
225	(A)--V	1.52976	2.67475
226	(A)--V	1.57307	2.68107
227	(A)--V	1.58396	2.72155
228	(A)--V	1.59324	2.61482
229	(A)--V	1.60878	2.76207
230	(A)--V	1.62995	2.72004
231	(A)--V	1.64512	2.75545
232	(A)--V	1.66276	2.81254
233	(A)--V	1.66495	2.82336
234	(A)--V	1.68908	2.82685
235	(A)--V	1.69882	2.90030
236	(A)--V	1.72452	2.91324
237	(A)--V	1.72970	3.14530
238	(A)--V	1.73725	2.93160
239	(A)--V	1.74530	2.96182
240	(A)--V	1.75834	2.97436
241	(A)--V	1.76362	3.07135
242	(A)--V	1.76868	3.04799
243	(A)--V	1.77636	3.09742
244	(A)--V	1.79121	2.97832
245	(A)--V	1.79755	3.01829
246	(A)--V	1.80395	3.12972
247	(A)--V	1.81970	3.03476
248	(A)--V	1.83036	3.05119
249	(A)--V	1.83625	3.07569
250	(A)--V	1.84822	3.10483
251	(A)--V	1.85608	3.18355

252	(A)--V	1.85851	3.18712
253	(A)--V	1.87180	3.27880
254	(A)--V	1.88053	3.18055
255	(A)--V	1.88876	3.22952
256	(A)--V	1.88986	3.18468
257	(A)--V	1.90833	3.19460
258	(A)--V	1.91628	3.19455
259	(A)--V	1.92768	3.26805
260	(A)--V	1.93161	3.08016
261	(A)--V	1.93620	3.21674
262	(A)--V	1.93950	3.25771
263	(A)--V	1.94536	3.26103
264	(A)--V	1.96169	3.20082
265	(A)--V	1.98006	3.28919
266	(A)--V	1.98805	3.29575
267	(A)--V	1.99280	3.23893
268	(A)--V	1.99962	3.21609
269	(A)--V	2.00791	3.14958
270	(A)--V	2.01235	3.26228
271	(A)--V	2.03438	3.29970
272	(A)--V	2.04453	3.30331
273	(A)--V	2.05716	3.29364
274	(A)--V	2.06131	3.33917
275	(A)--V	2.06402	3.08650
276	(A)--V	2.08699	3.41346
277	(A)--V	2.09556	3.34936
278	(A)--V	2.10402	3.35838
279	(A)--V	2.10838	3.32238
280	(A)--V	2.12009	3.34004
281	(A)--V	2.13020	3.35882
282	(A)--V	2.13756	3.35336
283	(A)--V	2.14582	3.37699
284	(A)--V	2.17297	3.33612
285	(A)--V	2.19418	3.40761
286	(A)--V	2.20702	3.45228
287	(A)--V	2.21583	3.46230
288	(A)--V	2.22510	3.41451
289	(A)--V	2.24104	3.30999
290	(A)--V	2.25418	3.40332
291	(A)--V	2.26205	3.31328
292	(A)--V	2.26327	3.35690
293	(A)--V	2.26898	3.43664
294	(A)--V	2.27729	3.46444

295	(A)--V	2.29316	3.52927
296	(A)--V	2.30047	3.41651
297	(A)--V	2.31080	3.51688
298	(A)--V	2.32400	3.51128
299	(A)--V	2.33839	3.59930
300	(A)--V	2.35023	3.58985
301	(A)--V	2.36520	3.50162
302	(A)--V	2.36999	3.50947
303	(A)--V	2.37715	3.56447
304	(A)--V	2.37982	3.56139
305	(A)--V	2.39033	3.45694
306	(A)--V	2.40388	3.59991
307	(A)--V	2.41115	3.63607
308	(A)--V	2.43035	3.63175
309	(A)--V	2.43379	3.55090
310	(A)--V	2.44895	3.68638
311	(A)--V	2.45103	3.60305
312	(A)--V	2.47757	3.76750
313	(A)--V	2.48714	3.72862
314	(A)--V	2.50323	3.59799
315	(A)--V	2.50906	3.70798
316	(A)--V	2.52160	3.75088
317	(A)--V	2.52616	3.69495
318	(A)--V	2.54476	3.81648
319	(A)--V	2.56180	3.81823
320	(A)--V	2.56310	3.77987
321	(A)--V	2.56919	3.67507
322	(A)--V	2.57867	3.81549
323	(A)--V	2.58952	3.74570
324	(A)--V	2.59423	3.72691
325	(A)--V	2.60242	3.77291
326	(A)--V	2.62122	3.73613
327	(A)--V	2.64115	3.81921
328	(A)--V	2.64830	3.79420
329	(A)--V	2.65871	3.88205
330	(A)--V	2.66649	3.80496
331	(A)--V	2.67966	3.75964
332	(A)--V	2.70092	3.89561
333	(A)--V	2.71246	3.90608
334	(A)--V	2.71421	3.91859
335	(A)--V	2.72128	3.87675
336	(A)--V	2.73709	4.05981
337	(A)--V	2.74466	3.86917

338	(A)--V	2.75251	3.94384
339	(A)--V	2.75958	3.98703
340	(A)--V	2.76524	3.99259
341	(A)--V	2.77329	3.97922
342	(A)--V	2.78331	3.98932
343	(A)--V	2.78955	4.00464
344	(A)--V	2.80575	4.05486
345	(A)--V	2.80924	4.01404
346	(A)--V	2.81916	4.16094
347	(A)--V	2.83807	4.01097
348	(A)--V	2.84105	4.02002
349	(A)--V	2.85561	3.98565
350	(A)--V	2.86316	4.07471
351	(A)--V	2.88062	4.04927
352	(A)--V	2.89037	4.10247
353	(A)--V	2.89742	4.08093
354	(A)--V	2.91526	4.23372
355	(A)--V	2.93641	4.06612
356	(A)--V	2.93875	4.37791
357	(A)--V	2.95962	4.21149
358	(A)--V	2.96724	4.34301
359	(A)--V	2.97874	4.23301
360	(A)--V	3.00352	4.24945
361	(A)--V	3.02642	4.47412
362	(A)--V	3.04563	4.84365
363	(A)--V	3.05013	4.35551
364	(A)--V	3.06944	4.44395
365	(A)--V	3.10601	4.65813
366	(A)--V	3.13930	4.59906
367	(A)--V	3.20568	4.93107
368	(A)--V	3.21293	4.94288
369	(A)--V	3.24115	4.91881
370	(A)--V	3.24730	4.94299
371	(A)--V	3.28109	5.01086
372	(A)--V	3.29960	5.00997
373	(A)--V	3.30797	5.05148
374	(A)--V	3.32295	4.99936
375	(A)--V	3.34205	5.00200
376	(A)--V	3.35628	5.02073
377	(A)--V	3.37483	5.06493
378	(A)--V	3.42184	5.59367
379	(A)--V	3.42944	5.09289
380	(A)--V	3.44789	5.07503

```
   381  (A)--V       3.45766   5.15805
   382  (A)--V       3.46637   5.30773
   383  (A)--V       3.47835   5.20575
   384  (A)--V       3.48938   5.31086
   385  (A)--V       3.50299   5.09584
   386  (A)--V       3.50585   5.15234
   387  (A)--V       3.51802   5.12273
   388  (A)--V       3.53769   5.16745
   389  (A)--V       3.56766   5.19178
   390  (A)--V       3.78521   5.67285
   391  (A)--V       4.06040  10.02492
   392  (A)--V       4.14593  10.16418
   393  (A)--V       4.16478  10.18705
   394  (A)--V       4.16994  10.25959
   395  (A)--V       4.24807  10.26373
   396  (A)--V       4.30512  10.33259
   397  (A)--V       4.37180  10.19670
   398  (A)--V       4.38373  10.16349
   399  (A)--V       4.41779  10.30050
   400  (A)--V       4.44854  10.16036
   401  (A)--V       4.50972  10.56646
   402  (A)--V       4.52135  10.24473
   403  (A)--V       4.58020  10.41390
   404  (A)--V       4.62809  10.41954
   405  (A)--V       4.69075  10.53628
   406  (A)--V       4.72712  10.49885
   407  (A)--V       4.79960  10.87775
   408  (A)--V       4.84015  10.83684
   409  (A)--V       4.87686  10.79196
   410  (A)--V       5.02877  11.46615
 Total kinetic energy from orbitals= 8.416414537699D+02
 No NMR shielding tensors so no spin-rotation constants.
 Leave Link  601 at Thu Sep 29 22:54:55 2011, MaxMem= 1207959552 cpu:
28.3
 (Enter /usr/local/packages/g03/l9999.exe)

 This type of calculation cannot be archived.


 Job cpu time:  0 days  0 hours  2 minutes 17.8 seconds.
 File lengths (MBytes):  RWF=     29 Int=      0 D2E=      0 Chk=     22 Scr=      1
 Normal termination of Gaussian 03 at Thu Sep 29 22:55:08 2011.
```

APPENDIX E

ESTROGENIC POTENTIAL ANALYSIS

This section contains the visual interpretation of the tabular analysis done for estrogenic potential in section 3.4

Figure 18: Estrogenic Potential: Direct Metabolites

Figure 19: Estrogenic Potential: 2OH-EE_2 pathway

Figure 20: Estrogenic Potential: 6HCYC-EE_2 pathway

Table 4: Estrogenic Potential analysis: Steroidal Estrogens and Sulfate Conjugates

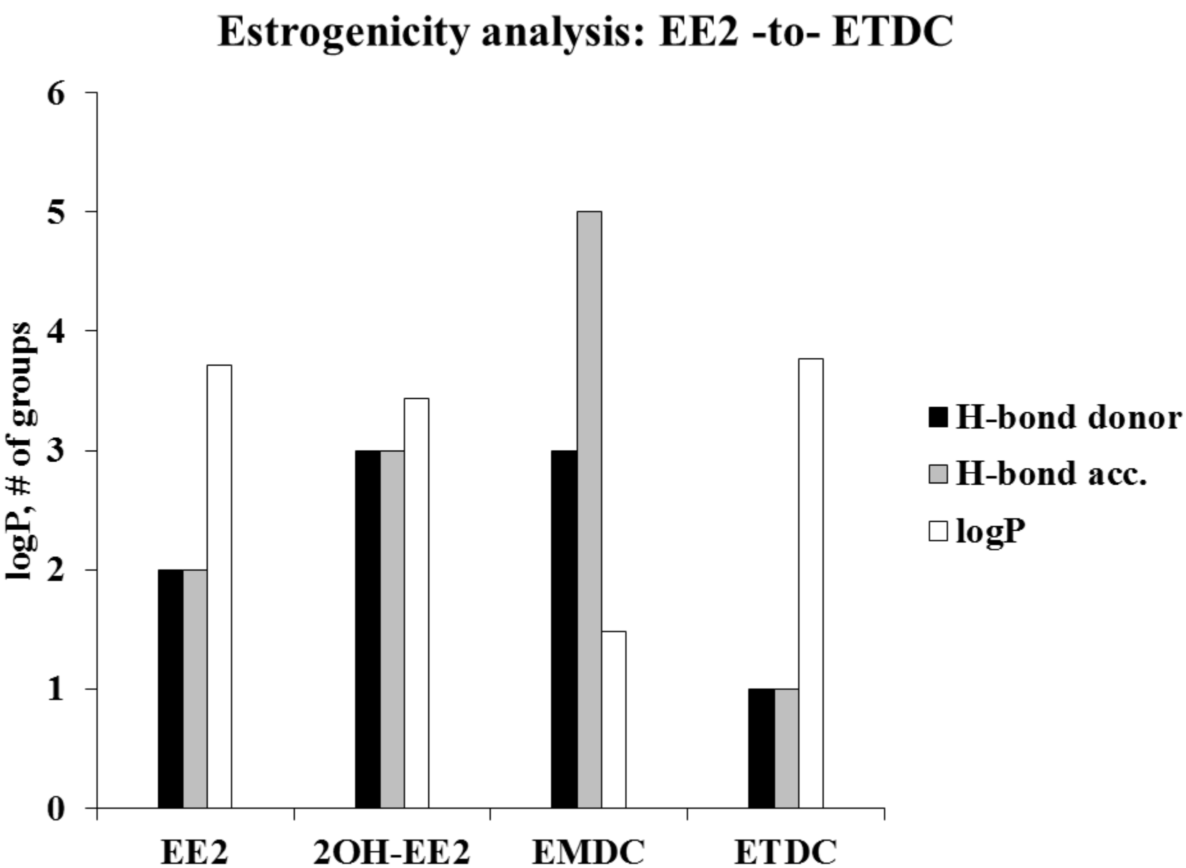

Figure 18. Estrogenic Potential: Direct Metabolites

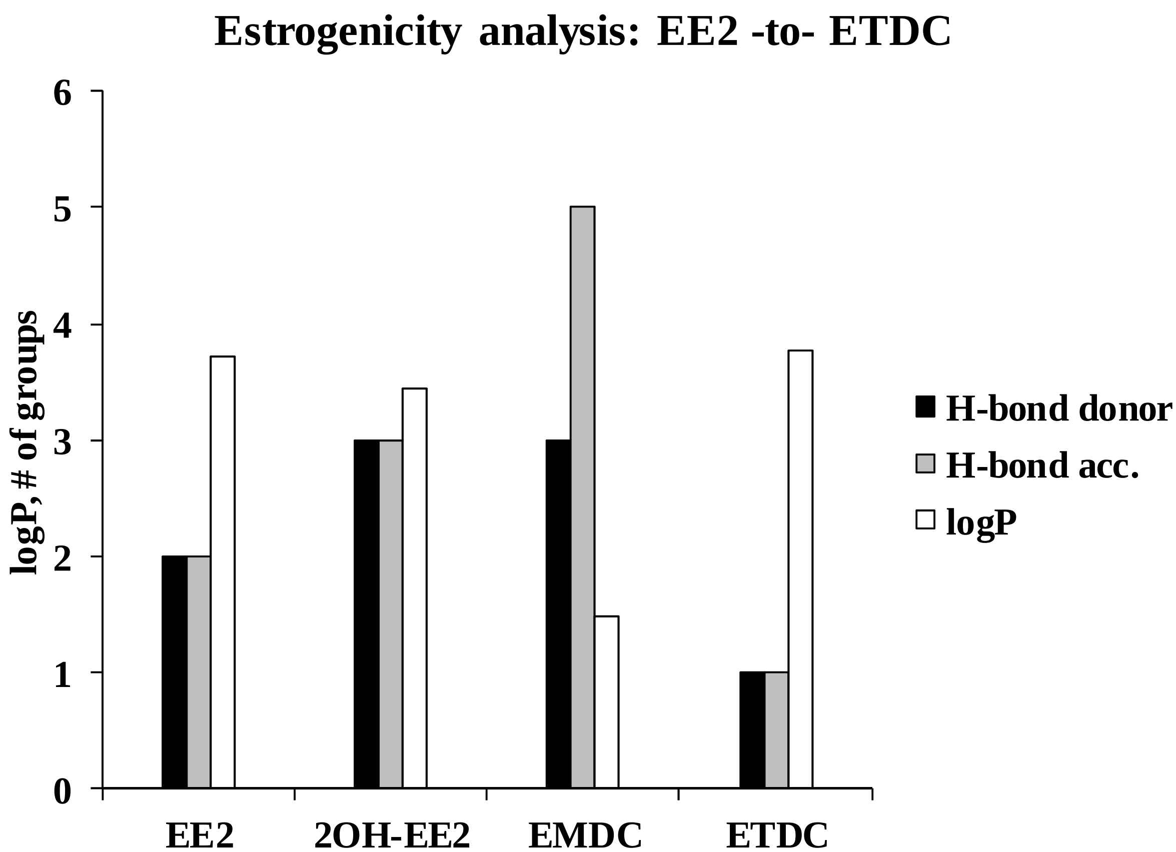

Figure 19. Estrogenic Potential: 2OH-EE_2 pathway

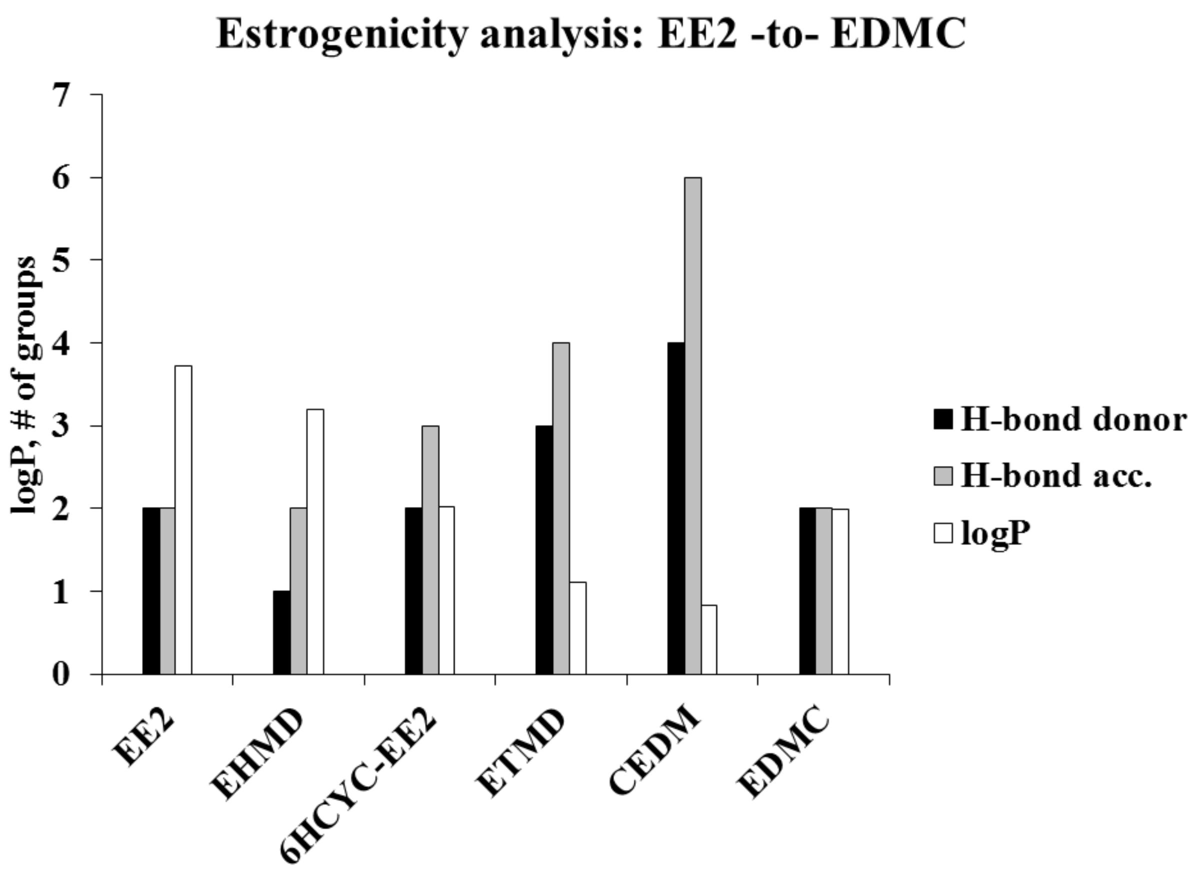

Figure 20. Estrogenic Potential: 6HCYC-EE_2 pathway

The following table is an estrogenic potential analysis for the natural steroidal estrogens and their sulfate conjugates.

Table 4. Estrogenic potential analysis of steroidal estrogens and sulfate conjugates

Compound	H-bond donors	H-bond acceptors	logP	Change in potential
E_1	1	2	4.54	Slight decrease
SE_1	1	5	3.78	Slightly more water soluble
E_2	2	2	3.71	Decrease
SE_2	2	5	2.95	More water soluble
EE_2	2	2	3.72	Decrease
SEE_2	2	5	2.96	More water soluble
E_3	3	3	2.64	Substantial decrease
SE_3	3	6	1.88	More water soluble

This table shows the consistency in the decrease in estrogenic potential with the occurrence of sulfonation. The order for estrogenic potential based on these results would be $EE_2 \geq E_2 > E_1 > E_3$. EE_2 has a higher hydrophobicity than E_2 because of the ethinyl group on ring D. E_2 has more hydrogen bond donor groups than E_1. E_3 has an extremely low hydrophobicity making it significantly easier to excrete than the other steroidal estrogens and thus less active. The estrogenic potential of each metabolite and parent compound has been analyzed and compared to known processes for removing estrogenicity to determine the potential remaining in each metabolite to exert estrogenic activity.

APPENDIX F

COMPLETE BIOLOGICAL METABOLITE TABLE

This table contains all metabolites analyzed during this study for FED analysis. It includes IUPAC names as they appear in Chemoffice software, molecular formulas, weights and abbreviations.

Table 5: 2OH-EE_2 pathway

Table 6: 6HCYC-EE_2 pathway

Table 7: SO_4-EE_2

Table 5. 2OH-EE_2 pathway information

ABBR.	FIGURE	IUPAC	MW
EE_2	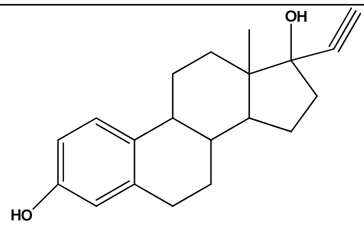	17-ETHYNYL-13-METHYL-7,8,9,11,12,13,14,15,16,17-DECAHYDRO-6H-CYCLOPENTA[A]PHENANTHRENE-3,17-DIOL	296.40
2OH-EE_2	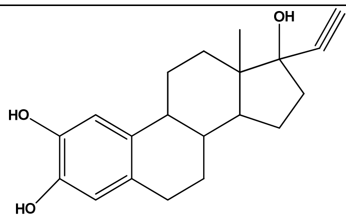	17-ETHYNYL-13-METHYL-7,8,9,11,12,13,14,15,16,17-DECAHYDRO-6H-CYCLOPENTA[A]PHENANTHRENE-2,3,17-TRIOL	312.40
EMDC	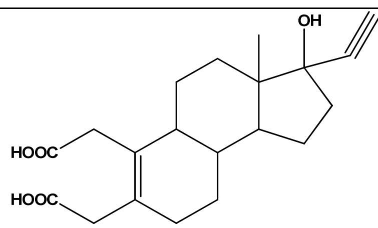	2,2'-(3-ETHYNYL-3-HYDROXY-3A-METHYL-2,3,3A,4,5,5A,8,9,9A,9B-DECAHYDRO-1H-CYCLOPENTA[A]NAPHTHALENE-6,7-DIYL)DIACETIC ACID	346.42
ETDC	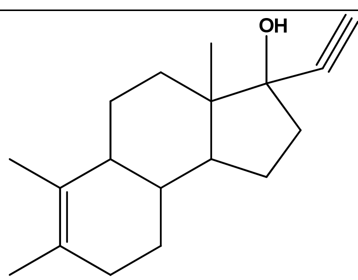	3-ETHYNYL-3A,6,7-TRIMETHYL-2,3,3A,4,5,5A,8,9,9A,9B-DECAHYDRO-1H-CYCLOPENTA[A]NAPHTHALEN-3-OL	258.40

Table 6. 6HCYC-EE_2 pathway information

ABBR.	FIGURE	IUPAC	MW
EHMD	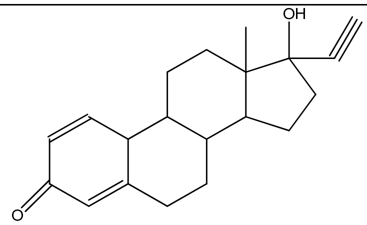	17-ETHYNYL-17-HYDROXY-13-METHYL-6,7,8,9,10,11,12,13,14,15,16,17-DODECAHYDRO-3H-CYCLOPENTA[A]PHENANTHREN-3-ONE	296.40
6HCYC-EE_2	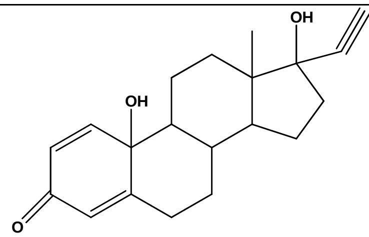	17-ETHYNYL-10,17-DIHYDROXY-13-METHYL-6,7,8,9,10,11,12,13,14,15,16,17-DODECAHYDRO-3H-CYCLOPENTA[A]PHENANTHREN-3-ONE	312.40
ETMD	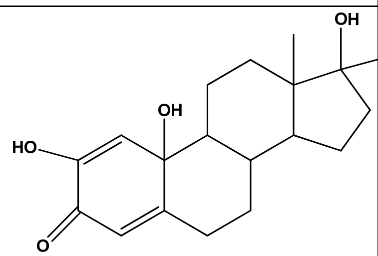	17-ETHYNYL-2,10,17-TRIHYDROXY-13-METHYL-6,7,8,9,10,11,12,13,14,15,16,17-DODECAHYDRO-3H-CYCLOPENTA[A]PHENANTHREN-3-ONE	328.40
CEDM	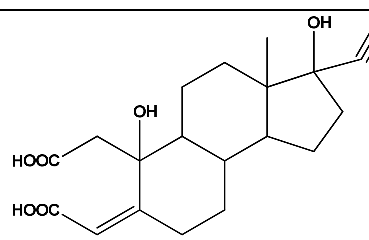	(Z)-2-(6-(CARBOXYMETHYL)-3-ETHYNYL-3,6-DIHYDROXY-3A-METHYLOCTAHYDRO-1H-CYCLOPENTA[A]NAPHTHALEN-7(2H,8H,9BH)-YLIDENE)ACETIC ACID	362.42
EDMC	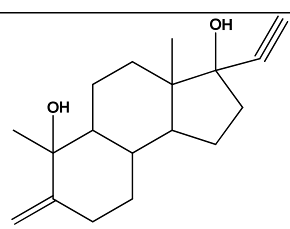	3-ETHYNYL-3A,6-DIMETHYL-7-METHYLENEDODECAHYDRO-1H-CYCLOPENTA[A]NAPHTHALENE-3,6-DIOL	274.40

Table 7. SO_4-EE_2 pathway information

ABBR.	FIGURE	IUPAC	MW
SO_4-EE_2	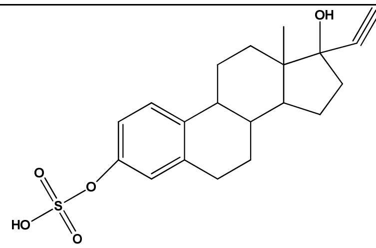	17-ETHYNYL-17-HYDROXY-13-METHYL-7,8,9,11,12,13,14,15,16,17-DECAHYDRO-6H-CYCLOPENTA[A]PHENANTHREN-3-YL HYDROGEN SULFATE	376.47

BIBLIOGRAPHY

Aldercreutz, H.; Fotsis, T.; Bannwart, C.; Hkmklkinen, E.; Bloigu, S.; Ollus, A. Urinary Estrogen Profile Determination in Young Finnish Vegetarian and Omnivorous Women. Journal of Steroidal Biochemistry. 2006, 24 (1), 289-296

Andersen, H.; Siegrist, H.; Halling-Sorensen, B. Ternes, T. A.; Fate of Estrogens in Municipal sewate treatment plant. Environ. Sci. and Technol., 2003,37, 18, 4021-4026

Baronti, C.; Curini, R.; D'Ascenzo, G.; Corcia, A. D.; Gentili, A.; Samperi, R. Monitoring natural and synthetic estrogens at activated sludge sewage treatment plants and in a receiving river. Environ Sci. and Technol. 2000, 34, 5059-5066

Brzostowicz, P. C.; Walters D. M.; Jackson, R. E.; Halsey, K. H.; Ni H.; Rouviere, P. E. Proposed involvement of soluble methane monooxygenase homologue in the cyclohexane dependent growth of a new Brachymonas species. Environ. Microbiol. 2005, 7, 179

Buikema jr., A. L.; Mcginniss, M. J.; Cairns Jr., J. Phenolics in aquatic ecosystems: A selected review of recent literature. Marine Environment Research. 1979, 2, 2, 87-181

Casellas, M.; Grifoll M.; Bayona, J. M.; Solanas, A. M. New metabolites in the degradation of fluorine by Arthrobacter sp. Strain F101, Appl. Environ, Microbiol. 1997, 63, 819

Cramers, C. J. Essentials of Computational Chemistry: Theories and Models. John Wiley & Sons. 2002

Dean-Ross, D.; Moody, J. D.; Freeman, J. P.; Doerge, D. R.; Cerniglia, C. E. Metabolism of anthracene by a Rhodococcus species. FEMS Microbiol Lett. 2001, 204, 205

Della-Greca, M.; Pinto, B.; Pistillo, P. Pollio, A.; Previtera, L.; Temussi, F. Biotransformation of ethinylestradiol by microalgae. Chemosphere. 2008, 70, 2047-2053

Dytczak, M.A.; Londry, K.L.; Oleszkiewwicz, J.A. Transformation of estrogens in nitrifying sludge under aerobic and alternating anoxic/aerobic conditions. 79th Annual Water Environment Federation Technical Exposition and Conference, Dallas, TX, October 2006.

Fang, H.; Tong, W.; Shi,L. M.; Blair, R.; Perkins, R.; Branham, W.; Hass, B. S.; Xie, Q.; Dial, S. L.; Moland, C. L.; Sheehan D. M. Structure-Activity Relationships for a Large Diverse Set of Natural, Synthetic, and Environmental Estrogens. Chem. Res. Toxicol, 2001, 14, 280-294

Fukui, K.; Yonezawa, T.; Shingu, H. A molecular orbital theory of reactivity in aromatic hydrocarbons. J. Chem. Phys., 1952, 20, 4, 722-725

Gaulke, L. S.; Strand, S.E.; Kalhorn, T.F.; Stensel, H.D. 17α-ethinylestradiol Transformation via Abiotic Nitration in the Presence of Ammonia Oxidizing Bacteria. Environ. Sci. and Technol. 2008, 42(20), 7622-7627.

Gentili, A.; Perret, D.; Marchese, S.; Mastropasqua, R.; Curini, R.; Di Corcia, A. Analysis of free estrogens and their conjugates in sewage and river waters by solid-phase extraction then liquid chromatography-electrospray-tandem mass spectrometry. Chromatogr. 2002, 56, 25-32.

Gibson, R.; Tyler, C. R.; Hill, E. M. Analytical methodology for the identification of estrogenic contaminants in fish bile. Journal of Chromatography A (2005) 1066, 33-40

Gusseme, B. D.; Pycke, B.; Hennebel, T.l Marcoen, A.; Vlaeminck, S. E.; Noppe, H.; Boon, N.l Verstraete, W. Biological removal of 17α-ethinylestradiol by a nitrifier enrichment culture in a membrane bioreactor. Water Research. 2009, 43, 2493-2503

Haiyan, R.; Shulan, J.; Naeem ud din Ahmad, Dao, W. and Chengwu, C. Degradation characteristics and metabolic pathway of 17α-ethynylestradiol by Sphingobacterium sp. JCR5. Chemosphere. 2007, 66(2), 340-346.

Hay, A. G.; Focht D. D. Cometabolism of 1,1-dichloro-2,2-bis(4-chlorophenyl)ethylene by Pseudomonas acidovorans M3GY grown on biphenyl. Appl. Environ, Microbiol. 1998, 64, 2141

Huang, C. H. and Sedlak, D. L. Analysis of estrogenic hormones in municipal wastewater effluent and surface water using enzyme-linked immunosrbent assay and gas chromatography/tandem mass spectrometry. Environmental Toxicology and Chemistry, 2001, 20, 1, 133-139

Hutchins, S. R.; White, M. V.; Hudson, F. M.; Fine, D. D. Analysis of Lagoon samples from different concentrated animal feeding operations for estrogens and estrogen conjugates. Environ Sci. and Technol. 2007, 41, 738-744

Kamath A. V.; Vaidyanathan C. S. New pathway for the biodegradation of indole by Aspergillus niger. Appl. Environ, Microbiol. 1990, 56, 275

Khunjar, W.O.; Mackintosh S.; Skotnicka-Pitak, J.; Baik S.; Aga, D.; and Love, N.G. Elucidating the Role of Ammonia Oxidizing Bacteria versus Heterotrophic Bacteria during the Biotransformation of 17α-ethinylestradiol and Trimethoprim. Environmental Science and Technol. 2011. 45, 3605-3612

Kolpin, D.; Furlong, E.; Meyer, M.; Thurman, E.; Zaugg, S.; Barber, L.; Buxton, H. Pharmaceuticals, hormones, and other organic wastewater contaminants in U.S. streams, 1999-2000: A national reconnaissance. Environ. Sci. and Technol. 2002, 36(6), 1202-1211

Kotov, A.; Falany, J. L.; Wang, J.; Falany, C. N. Regulation of estrogen activity by sulfation in human Ishikawak endometrial adenocarcinoma cells. Journal of Steroidal Biochemistry. 1999 68 (3-4), 137-144

Kuch, H. M. and Ballschmiter, K. Determination of endocrine-disrupting phenolic compounds and estrogens in surface and drinking water by HRGC-(NCI)-MS in the pictogram per liter range. Environ Sci. and Technol. 2001, 35, 3201-3206

Lee, B.-D.; Iso, M.; Hosomi, M. Prediction of Fenton oxidation positions in polycyclic aromatic hydrocarbons by Frontier electron density. Chemosphere. 2001, 42, 431-435.

Lee, Y.; Escher, B. I.; Von Gunten, U. Efficient removal of estrogenic activity during oxidative treatment of waters containing steroid estrogens. Environ. Sci. and Technol. 2008, 42, 17, 6333-6339

Lehninger, A.; Nelson, D.; Cox, M. Principles of Biochemistry. 2nd Ed., Worth Publishers, New York, N.Y. 1999

Lipinski, C. A.; Lombardo, F.; Dominy, B. W.; Feeney, P. J. Experimental and computational approaches to estimate solubility and permeability in drug discovery and development settings. Advanced Drug Delivery Reviews, 2001, 46, 3-26

Liu, G.; Li, X.; Zhao, J.; Horikoshi, S.; Hidaka, H. Photooxidation mechanism of dye alizarin red in TiO2 dispersions under visible illumination: an experimental and theoretical examination. Journal of Molecular Catalysis A: Chemical. 2000, 153, 221-229

Marvin 5.2, 2009, ChemAxon (http://www.chemaxon.com)

Nagy, P. I.; Fabian W. M. F. Theoretical study of the enol imine – enaminone tautomeric equilibrium in organic solvents. J. Phys Chem B. 2006, 110, 25026-25032.

Nakazawa, T.; Hayashi E. Phthalate and 4-hydroxyphthalate metabolism in Pseudomonas testosterone: Purification and properties of 4,5 dihydroxyphthalate decarboxylase. Appl. Environ, Microbiol. 1978, 36, 264

Nishikawa, J.; Salto, K.; Goto, J.; Dakeyama, F.; Matsuo, M.; Nishihara, T. New screening methods for chemicals with hormonal activities using interaction of nuclear hormone receptor with coactivator. Toxicology and Applied Pharmacology, 1999, 154, 76-83

Nosova, T.; Jousimies-Summer, H.; Kaihovaara, P.; Jokelainen, K.; Heine, R.; Salaspuro, M. Characteristics of alcohol dehydrogenases of certain aerobic bacteria representing human colonic flora. Alcohol Clin. Exp. Res. 1997, 21, 489

Ohko, Y.; Iuchi, K.I.; Niwa, C.; Tatsuma, T.; Nakashima, T.; Iguchi, T.; Kubota, Y.; Fujishima, A. 17β-estradiol degradation by TiO2 photocatalysis as a means of reducing estrogenic activity. Environ. Sci. and Technol. 2002, 36(19):4175-4181.

Ohura, T.; Amagai, T.; Sugiyama, T.; Fusaya, M.; Matsushita, H. Occurrence, profiles, and photostabilities of chlorinated polycyclic aromatic hydrocarbons associated with particulates in urban Air. Environ. Sci. and Technol. 2005, 39(1):2045-2054.

Olsen, R. H.; Kukor, J. J.; Kaphammer, B. A novel toluene-3-monooxygenase pathway cloned from Pseudomonas pickettii PK01. J. Bacteriol., 1994, 176, 3749

Parkkonen, J.; Larsson, D.; Adolfsson-Erici, M.; Pettersson, M.; Berg, A.; Olsson, P.; Förlin, L. . Contraceptive pill residues in sewage effluent are estrogenic to fish. Marine Environmental Research. 2000, 50(1-5), 198.

Pawlowski, S.; Aerle, R. V.; Tyler, C. R.; Braunbeck, T. Effects of 17α-ethinylestradiol in a fathead minnow (Pimephales promelas) gonadal recrudescence assay. Ecotox. and Environ. Safety. 2004, 57, 330-345

Poirier, R.; Kari, R.

Purdom, C.E.; Hardiman, P. A.; Bye, V. J.; Eno, N. C.; Tyler C. R.; Sumpter J.P. Estrogenic effects of effluents from sewage treatment works. Chemical Ecol. 1994, 8, 275-285

Routledge, E. J.; Sheahan, D.; Desbrow, C.; Brighty, G. C.; Waldock, M.; Sumpter, J. P. Identification of estrogenic chemicals in STW effluent. 2. In vivo responses in trout and roach. Environ. Sci. Technol. 1998, 32, 1559-1565.

Routledge, E. J. and Sumpter, J. P. Estrogenic activity of Surfactants and some of their degradation products assesses using a recombinant yeast screen. Environmental Toxicology and Chemistry. 1996 15, 3, 241-248

Saliner, A. G.; Amat, L.; Carbo-Dorca, R.; Schultz, T. W.; Cronin, M. T. D. Molecular quantum similarity analysis of estrogenic activity, J. of Chemical Information Science,, 2003, 43, 1166-1176

Schultz, T. W.; Sinks, G. D.; Cronin M. T. D. Structure-Activity Relationships for gene activation Oestrogenicity: Evaluation of a diverse set of aromatic chemicals. Environ. Toxicol. 2002, 17, 14-23

Shi, J.; Fujisawa, S.; Nakai, S.; and Hosomi, M. Biodegradation of natural and synthetic estrogen by nitrifying activated sludge and ammonia-oxidizing bacterium Nitrosomonas europaea. Water Research. 2004, 38(9), 2323-2330.

Shilling, A. D. and Williams, D. E. Determining Relative Estrogenicity by quantifying vitellogenin induction in ranbow trout liver slices. Toxicology and Applied Pharmacology, 2000, 164, 330-335

Steffan, R. J.; McClay, K.; Vainberg, S.; Condee, C. W.; Zhang, D. Biodegradation of the gasoline oxygenates methyl tert-butyl ether, ethyl tert-butyl ether, and tert-amyl methyl ether by propane-oxidizing bacteria. Appl. Environ, Microbiol. 1997, 61, 4216

Waller, C. L.; Oprea, T. I.; Chae, K.; Park, H. K.; Korach, K. S.; Laws, S.C.; Wiese, T. E.; Kelce, W.R.; Gray, L. E. Ligand-based identification of environmental estrogens. Chem Res Toxicol. 1996, 9, 1240–1248.

Wang, G.; Xue, X.; Li, H.; Wu, F.; Deng N. β-Cyclodextrin-enhanced photo degradation of bis(4-hydroxyphenyl)ethane under UV irradiation. J. Molecular Catalysis A: Chemical, 2007, 276, 143-149

Yi, T.; Harper Jr. W.F. The Link between Nitrification and Biotransformation of 17α-Ethinylestradiol. Environ. Sci. Technol. 2007, 41, 4311-4316

Zamek-Gliszczynski, M. J.; Hoffmaster, K. A.; Nezasa, K.; Taliman, M. N.; Brower, K. L. Integration of hepatic drug transporters and phase II metabolizing enzymes: mechanisms of hepatic excretion of sulfate glucoronide and glutathione metabolites. European Journal of Pharmaceutical Science 2006, 27 (5), 447-86